From the Department of Clinical Neuroscience
Karolinska Institutet, Stockholm, Sweden

DEVELOPMENT OF CANNABINOID SUBTYPE-1 (CB1) RECEPTOR LIGANDS FOR PET

Sean R. Donohue

Karolinska Institutet

Stockholm 2008

Published by Karolinska Institutet. Printed by Karolinska University Press

ISBN 978-91-7409-029-1

ABSTRACT

Introduction. Abnormalities in brain cannabinoid subtype-1 (CB_1) receptor concentrations and/or signaling pathways may be involved in a variety of psychiatric and neurodegenerative disorders. There is a strong need to image and quantify brain CB_1 receptor concentrations in living humans under baseline and diseased conditions. When this project began there were no CB_1 receptor radioligands suitable for in vivo imaging with PET. The overall aim of this project was the development of CB_1 receptor PET radioligands as tools for neuropsychiatric research and drug development.
Methods. 1,5-Diarylpyrazole and 3,4-diarylpyrazoline CB_1 receptor ligands were prepared and assayed in vitro for affinity/potency and selectivity at CB_1 receptors. A facile and selective approach to the synthesis of 1,5-diarylpyrazoles was identified to assist in advancing SAR in this class. Three high-potency [^{11}C]1,5-diarylpyrazoles ([^{11}C]**12**, [^{11}C]**14** and [^{11}C]**17**) were synthesized from their *O*-desmethyl precursors (**23**–**25**) and [^{11}C]iodomethane and purified with HPLC. PipISB (**26**) was radiolabeled in either of two positions, with [^{11}C]carbon monoxide or with [^{18}F]4-fluoro-benzyl bromide as labeling agent. Candidate radioligands ([^{11}C]**27** and [^{18}F]**28**–**30**) from the 1,5-diphenyl-pyrrolidin-2-one platform of [^{11}C]MePPEP ([^{11}C]**16**) were prepared from *O*-desmethyl precursor (**31** or **32**) with [^{11}C]iodomethane, [^{18}F]FCH_2Br, [^{18}F]FCD_2Br or [^{18}F]$F(CH_2)_2Br$ as labeling agents. A promising racemic [^{11}C]3,4-diarylpyrazoline ([^{11}C](±)-**33**), its eutomer ([^{11}C](–)-**33**) and distomer ([^{11}C](+)-**33**) were radiolabeled with [^{11}C]HCN using a custom-made remotely-controlled apparatus. With the exceptions of [^{11}C]**27** and [^{18}F]**28**–**30**, each candidate radioligand was injected into monkey and investigated with PET imaging.
Results and Discussion. Ligands (**12**–**14**, **17**, (±)-**33**) and their *O*-desmethyl precursors (**23**–**25**, **34**) were synthesized efficiently and in useful chemical yields. The achieved RCYs, SRs and purities of each radioligand were adequate for future investigation in vivo with PET imaging. After injection into monkey, two 1,5-diarylpyrazoles, [^{11}C]**12** and [^{11}C]**17**, gave some receptor-specific signal in brain but were likely contaminated with brain-penetrating radiometabolites and were therefore unsuitable for PET imaging. The third, [^{11}C]**14**, gave an appreciable receptor-specific signal and fast brain washout. The success of [^{11}C]**14** is likely related to the favorable metabolism conferred by the nitrile substituent in the 4-position of the pyrazole ring. [^{11}C]**26** and [^{18}F]**26** showed high CB_1 receptor-specific binding in monkey brain in vivo and merit further investigation as prospective PET radioligands in humans. [^{11}C](±)-**33** showed an appropriate regional brain distribution and its binding was selectively blocked by pre- or post treatment with a high dose of CB_1-selective ligand. After injection of [^{11}C](−)-**33**, there was high uptake and retention of radioactivity across brain according to the rank order of CB_1 receptor densities. The distomer, [^{11}C](+)-**33** failed to give a sustained CB_1 receptor-specific distribution.
Conclusion. From the work produced in this thesis, four radioligands ([^{11}C]**14**, [^{11}C]**26**, [^{18}F]**26** and [^{11}C](−)-**33**) appear promising for in vivo imaging of brain CB_1 receptors with PET in monkey. [^{11}C](−)-**33** is currently being considered for use in human subjects under a clinical protocol.

LIST OF PUBLICATIONS

I. Donohue, S. R.; Halldin, C.; Pike, V. W. Synthesis and structure-activity relationships (SARs) of 1,5-diarylpyrazole cannabinoid type-1 (CB_1) receptor ligands for potential use in molecular imaging. *Bioorg. Med. Chem.* **2006**, *14*, 3712–3720.

II. Donohue, S. R.; Halldin, C.; Pike, V. W. A facile and regioselective synthesis of rimonabant through an enamine-directed 1,3-dipolar cycloaddition. *Tetrahedron Lett.* **2008**, *49*, 2789–2791.

III. Donohue, S. R.; Zoghbi, S. S.; Yasuno, F.; Gourley, J. P.; Innis, R. B.; Halldin, C. and Pike, V. W. Radiosynthesis and evaluation in monkey of three ^{11}C-labelled 1,5-diarylpyrazoles as high potency candidate PET radioligands for cannabinoid subtype-1 (CB_1) receptors in brain. *Current Radiopharmaceuticals* **2008**, *1*, 93–102.

IV. Donohue, S. R.; Halldin, C.; Schou, M.; Hong, J.; Phebus, L.; Chernet, E.; Hitchcock, S. A.; Gardinier, K. M.; Ruley, K. M.; Krushinski, J. H.; Schaus, J.; Pike, V. W. Radiolabeling of a high potency cannabinoid subtype-1 receptor ligand, *N*-(4-fluoro-benzyl)-4-(3-(piperidin-1-yl)-indole-1-sulfonyl)benzamide (PipISB), with carbon-11 or fluorine-18. *J. Label. Compd. Radiopharm.* **2008**, *51*, 146–152

V. Finnema, S. J.; Donohue, S. R.; Zoghbi, S. S.; Brown, A. K.; Gulyás, B.; Innis R. B.; Halldin, C.; Pike, V. W. Evaluation in monkey of [^{11}C]PipISB and [^{18}F]PipISB as candidate radioligands for imaging brain cannabinoid type-1 (CB_1) receptors in vivo. *Synapse* **2008**, Manuscript (submitted).

VI. Donohue, S. R.; Krushinski, J. H.; Pike, V. W.; Chernet, E.; Chesterfield, A. K.; Felder, C. C.; Halldin, C.; Schaus, J. M. Synthesis, *ex vivo* evaluation and radiolabeling of potent 1,5-diphenyl-pyrrolidin-2-one cannabinoid subtype-1 (CB_1) receptor ligands as candidates for *in vivo* imaging. *J. Med. Chem.* **2008**, Manuscript (submitted).

VII. Donohue S. R.; Pike, V. W.; Finnema, S. J.; Truong, P.; Andersson, J.; Gulyás, B. and Halldin, C. Discovery and labeling of high affinity 3,4-diarylpyrazolines as candidate radioligands for *in vivo* imaging of cannabinoid subtype-1 (CB_1) receptors. *J. Med. Chem.* **2008**, Manuscript (submitted).

CONTENTS

LIST OF ABBREVIATIONS

AEA	Anandamide
2-AG	2-Arachidonoyl glycerol
AIDS	Aquired immune deficiency syndrome
AEA	Anandamide
BBB	Blood-brain barrier
BP	Binding potential
Bq	Bequerel
CB_1	Cannabinoid subtype-1
CB_2	Cannabinoid subtype-2
CB_3	Cannabinoid subtype-3
CN	Compound nucleus
CNS	Central nervous system
DCM	Dichloromethane
DME	1,2-Dimethoxyethane
DMF	*N*,*N*-Dimethyl-formamide
DMSO	Dimethyl sulfoxide
EOS	End of synthesis
EtOAc	Ethyl acetate
EU	European Union
FAAH	Fatty acid amide hydroxylase
FDA	Food and Drug Administration
GABA	γ-Aminobutyric acid
GPR55	G-protein coupled receptor-55
GTPγS	Guanosine-5'-(γ-thio)-triphosphate
HPLC	High-performance liquid chromatography
IND	Investigational New Drug
ISPB	4-(3-Cyclopentyl-indole-1-sulfonyl)-*N*-(tetrahydro-pyran-4-yl-methyl)-benzamide
IUPHAR	International Union of Pharmacology
LiHMDS	Lithium hexamethyldisilazide
K 2.2.2	4,7,13,16,21,24-Hexaoxa-1,10-diazabicyclo[8.8.8]hexacosane
KI	Karolinska Institutet
LogP	Logarithm of partition coefficient
MAP	Mitogen-activated protein
MeCN	Acetonitrile
mol	mole
MRI	Magnetic resonance imaging
MRS	Magnetic resonance spectroscopy
MS	Multiple sclerosis
NCA	No-carrier-added
NIH	National Institutes of Health
NIMH	National Institute of Mental Health
PET	Positron emission tomography
PipISB	*N*-(4-Fluoro-benzyl)-4-(3-(piperidin-1-yl)-indole-1-

	sulfonyl)benzamide
QMA	Quaternary methyl ammonium
RT	Room temperature
RCY	Radiochemical yield
SARs	Structure-activity relationships
SPECT	Single photon emission computed tomography
SR	Specific radioactivity
SUV	Standard uptake value
TAC	Time-activity curve
TEA	Triethylamine
Tf	Triflate
TFA	Trifluoroacetic acid
TRPV1	Transient receptor potential vanilloid-1
VOI	Volume of interest

1 INTRODUCTION

C*annabis sativa* (marijuana) is one of oldest known plant-derived therapeutics.[1] Its reported use dates back to that of a Chinese Emperor in 3000 B.C. In most early civilizations, *Cannabis* was a recommended treatment for pain, low appetite, nausea, fever and certain infections. The most common methods of *Cannabis* intake are inhalation or ingestion of dried leaves, extracts or resin. Certain negative effects such as psychological "high", drowsiness and memory impairment have limited contemporary therapeutic use and value.[1,2] The acute physiological "high" associated with *Cannabis* intake has also resulted in its considerable misuse as a recreational tool. Many countries now have strict regulations regarding the growth, distribution, sale and use of *Cannabis* or its extracts.

Despite the long history of use among certain cultures, mechanistic studies of the pharmacologically active compounds and their cellular receptors are of relatively recent origin. The studies represented in this thesis began with an investigation of a series of 1,5-diarylpyrazole candidate radioligands and their structure-activity relationships (SARs) and culminated in the discovery and labeling of a novel, high-affinity 3,4-diarylpyrazoline for in vivo imaging of brain cannabinoid subtype-1 receptors with PET (positron emission tomography).

This research involved the synthesis, radiolabeling and in vivo PET evaluation of several candidate CB_1 receptor radioligands. The work was carried-out at the Karolinska Institutet (KI) and National Institutes of Health (NIH) under the KI-NIH Graduate Partnership Program in Neuroscience.

1.1 CANNABINOIDS AND THEIR RECEPTORS

A systematic effort to elucidate the biologically active components of marijuana identified approximately 60 plant-derived compounds (phytocannabinoids) that exhibit cannabinoid like behavior in vitro and/or in vivo.[3] The isolation and structural determination of the main psychoactive phytocannabinoid was reported in 1964 by Gaoni and Mechoulam.[4] This compound was named Δ^9-tetrahydrocannabinol or Δ^{1}-tetrahydrocannabinol (**1**, Δ^9-THC, Figure 1) depending on the numbering system. Its absolute stereochemical configuration was reported in 1967 by the same investigators.[5]

Due to the inherently high lipophilicity of phytocannabinoids, their biological response was originally hypothesized to result from non-specific perturbation of membrane lipids. However, the isolation, structural identification and stereospecific pharmacology of **1** led investigators to believe in the existence of one or more specific receptors. A program at Pfizer, exploring the development of small molecule analgesics based on the template of **1,** identified 2-[(1*S*,2*R*,5*S*)-5-hydroxy-2-(3-hydroxypropyl)cyclohexyl]-5-(2-methyloctan-2-yl)phenol (CP 55,940, **2**, Figure 1) as a highly efficacious cannabinoid with relatively low lipophilicity.[6]

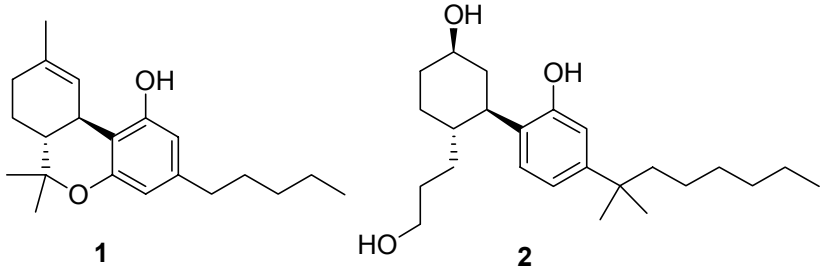

Figure 1. Structures of **Δ**^{9}-THC (**1**) and CP-55,940 (**2**).

The use of [^{3}H]**2** in vitro helped to identify the cannabinoid receptors more clearly, namely the cannabinoid sub-type-1 (CB_1) and sub-type-2 (CB_2) receptors.[7,8] Two CB_1 receptor spliced variants have also been identified, CB_{1A} and CB_{1B}.[9,10] The CB_1 receptor has been cloned from a variety of species and its amino acid sequence is highly conserved across species and exhibits 97% sequence homology.[11] The CB_2 receptor exhibits 48% homology with the CB_1 receptor.[11] There is also evidence for a cannabinoid type-3 (CB_3) receptor which may be the orphan G protein-coupled receptor 55 (GPR55)[12]. However, the International Union of Pharmacology (IUPAR) has not yet accepted GPR55 as a CB_3 receptor.

CB_1 receptors are one of the most abundant G-protein coupled receptors in the brain and have a concentration (B_{max}) of 1752 fmol/mg protein[13] in rat cerebellum. In comparison, dopamine-2 (D_2) receptors in the striatum have a B_{max} of 247 fmol/mg protein[14]. CB_1 receptors have their highest densities in the globus pallidus, substantia nigra, molecular layer of the cerebellum, cerebral cortex, striatum and hippocampus. Areas of the brain almost devoid of CB_1 receptor expression are the thalamus and pons.[15-17] CB_1 receptors are also expressed in certain peripheral tissues such as testis, ileum, urinary bladder and vas deferens.[11] CB_2 receptors are located mainly in tissues of the immune system, such as the macrophages of spleen, bone marrow, and pancreas, as well as at peripheral nerve terminals.[18,19] Low levels of CB_2 receptors have been found in brain in both neurons and glia. However, their physiological roles in the brain have not been fully elucidated.[20,21]

1.2 ENDOCANNABINOIDS

To date a few endogenous ligands have demonstrated binding to cannabinoid receptors. These include anandamide (AEA, **3**, Figure 2)[22], 2-arachidonoyl glycerol (2-AG, **4**, Figure 2)[23,24], 2-arachidonoyl glycerol ether[24], *O*-arachidonoyl ethanolamine (virodhamine)[25] and *N*-arachidonoyl dopamine[26,27]. Most of these ligands are derived from a polyunsaturated arachidonic acid-like platform. Two of the most thoroughly studied are **3** and **4**. In the brain, **3** is produced post-synaptically from a specific membrane phospholipid on demand following an influx of calcium ions caused by the neurotransmitter L-glutamate.[28] **3** is then released into the extracellular space where it binds to a pre-synaptic CB_1 receptor. It is believed that the primary role for pre-synaptic CB_1 receptors is to regulate the release of neurotransmitters such as γ-aminobutyric acid (GABA).[27] The enzyme, fatty acid amide hydroxylase (FAAH), controls extra-cellular concentrations of the endocannabinoids through hydrolysis of the amide bond, releasing arachidonate and choline.[28]

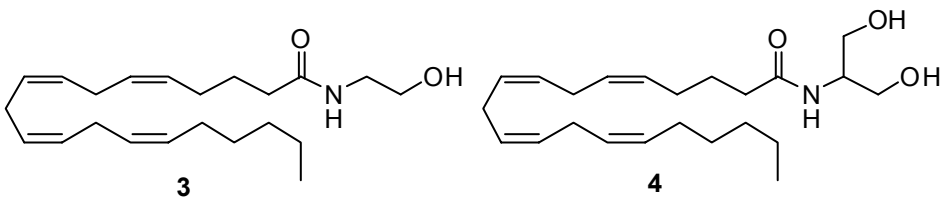

Figure 2. Structures of anandamide (**3**) and 2-arachidonoyl glycerol (**4**).

1.3 SIGNAL TRANSDUCTION VIA CANNABINOID RECEPTORS

Signaling via cannabinoid receptors is remarkably complex and a detailed description is outside the scope of this thesis. Briefly, agonist modulation of CB_1 receptors results in inhibition of adenylate cyclase activity through the $G_{i/\alpha}$ isoforms.[29] Paradoxically, stimulation of adenylate cyclase is also possible when there is simultaneous activation of CB_1 and dopamine receptors.[29] There is also evidence that activation of cannabinoid recepors is linked to modulation of intracellular calcium levels in brain neurons and well as activation of potassium channels.[30] A variety of mitogen-activated protein (MAP) kinases are activated by cannabinoid compounds.[31]

1.4 CB_1-RELATED NEUROPSYCHIATRIC DISORDERS AND PHARMACOTHERAPY

Brain CB_1 receptors may play roles in an array of psychiatric and neurodegenerative disorders. The linked disorders include anxiety[32], depression[33], addiction[34], chronic pain[35], Tourette's syndrome[35], multiple sclerosis (MS)[36], Parkinson's disease[37] and Huntington's disease[38]. Therapeutic intervention with CB_1 agonists has followed two approaches: 1) direct modulation by treatment with phytocannabinoids or chemically modified synthetic ligands; 2) indirect modulation of the endocanninoid system by interfering with biosynthetic/metabolic pathways or transport mechanisms.

Apart from cannabis, dronabinol (**1**, Marinol®), nabilone (Cesamet®) and Sativex® (*i.e.*, a mixture of **1** and cannabidiol) have been the most widely prescribed cannabinoid agonists for medical therapy.[39] **1** has proven to be useful for increasing the appetite of patients with cancer or aquired immune deficiency syndrome (AIDS)[40], reducing ocular pressure in patients with glaucoma[38], reducing ticks in patients with Tourette's syndrome[41] and relieving pain in patients with MS[36]. However, approximately 100 metabolites of **1** have been identified after ingestion in humans and 25 of these are thought to be bioactive. The complicated metabolism of **1** has made interpretation of its clinical trials difficult. Nabilone is a synthetic cannabinoid derived from the structure of **1** but has a more predictable outcome measure and produces a minimal psychological "high". It is primarily used as an antiemetic and treatment for neuropathic pain. Sativex® is a mouth spray for alleviating pain in patients with MS.

In 1994, Rinaldi-Carmona et al. at Sanofi-Aventis introduced rimonabant (**5**, Acompli® or Zimulti®, Figure 3)[42] as a high-affinity CB_1 receptor antagonist. **5** is now considered to be a CB_1 receptor inverse agonist. Since the introduction of **5**, several studies have evaluated the medical usefulness of CB_1 receptor inverse agonists or antagonists. These studies have found CB_1 receptor inverse agonists to be especially useful for the treatment of obesity[43] and smoking cessation[44]. After phase III clinal trials, **5** was approved in the European Union (EU) to treat the clinically obese. It was not however approved to help with smoking cessation. In the United States, **5** was not approved for sale by the Food and Drug Administration (FDA) due to unanswered concerns about its safety.

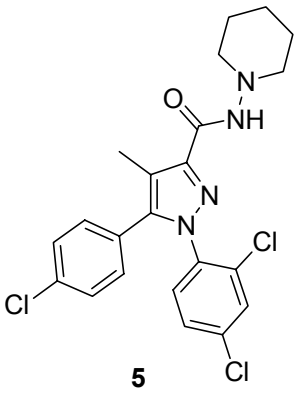

5

Figure 3. Structure of rimonabant (**5**).

1.5 TECHNIQUES FOR NEUROPSYCHIATRIC IMAGING IN VIVO

Imaging of brain neuroreceptor systems in living subjects can play a significant role in clinical research related to understanding neuropsychiatric conditions. Several "non-invasive" medical imaging techniques are available to clinical researchers. A few of these include magnetic resonance imaging (MRI), single photon emission computed tomography (SPECT) and positron emission tomography (PET). Each of these techniques has associated advantages and disadvantages. Selection of imaging technique for research purposes is often driven by consideration of the purpose of the project, access to equipment, availability of experienced personnel, and costs.[45]

Many psychiatric disorders are suspected to be driven by abnormalities in certain neuroreceptor/protein transporters, neurotransmitters and/or neuromodulator concentrations and receptor signaling pathways. In this case PET has the advantage over MRI in that it can selectively and qualitatively image low receptor densities and signaling pathways in diseased and non-diseased patients. PET relies on pre-administration of a radioactive source bound to a molecule tailored for a specific application. A cyclotron, radiochemistry facilities, coincidence detector (PET camera), data reconstruction software and biomathematical modeling are required to produce, receive, and interpret the data. If performing receptor binding studies, only PET and not MRI can be used because PET has higher sensitivity and therefore allows for low mass radioligand experiments. A high mass would saturate the available receptors and hence MRS, with lower mass sensitivity, cannot be used for this purpose. PET is superior to SPECT because a quantitative measurement can be made and sensitivity for radioactivity detection is higher.

The most commonly applied radioisotopes in PET imaging are carbon-11 (1.0 MeV, $t_{1/2}$ = 20.4 min) and fluorine-18 (0.6 MeV, $t_{1/2}$ = 109.7 min). As the name of the imaging technique implies, these neutron-deficient radionuclides undergo decay by emission of a positron. The positron is the "anti-matter" equivalent of an electron and has positive charge. After production, the positron will rapidly collide with a nearby electron and annihilate. The distance traveled by the positron before annihilation with a nearby electron is dictated by its kinetic energy. In PET, the imaging resolution can be inversely related to the positron kinetic energy. After positron annihilation two γ-photons (511 keV) are emitted at an angle of nearly 180^{o} and the resulting "line of coincidence" negates the need for a collimator.

The work presented in this thesis focused on the development of a radioligand for PET imaging of brain CB_1 receptors and applied the positron-emitters, carbon-11 and fluorine-18.

1.6 NUCLEAR REACTIONS

Carbon-11 and fluorine-18 are prepared from cyclotron-induced nuclear reactions. In such nuclear reactions, a high energy particle (e.g., an accelerated proton) is absorbed by a target nucleus forming a compound nucleus (CN) which then undergoes decay into a product nucleus. These reactions may be written as described below. The work described in this thesis will use shorthand notation. The most common and useful nuclear reactions for producing carbon-11 and fluorine-18 are $^{14}N(p,\alpha)^{11}C$ and $^{18}O(p,n)^{18}F$, respectively.

$$X + x \longrightarrow [CN] \longrightarrow Y + y$$

or in shorthand

$$X(x,y)Y$$

X = target nucleus
x = incident particle
Y = product nucleus
y = decay particle

The physics of nuclear reactions has been described elsewhere and a detailed description is outside the scope of this introduction.[46] Briefly, nuclear reactions producing carbon-11 and fluorine-18 are endothermic processes. This means that the incident particle must have sufficient energy for reaction to occur. Additional energy may be required for positively charged incident particles to overcome the Coulombic barrier at the target nucleus. A cyclotron is required to accelerate the incident particle to a necessary energy value. The type of nuclear reaction occurring and its productivity depend on the incident particle energy. Therefore, the energy of the incident particle is usually specified for PET nuclear reaction. To produce carbon-11 and fluorine-18 with protons, the energy is typically about 16 MeV but will depend on the available cyclotron. The overall yield (R) of a nuclear reaction is proportional to the intensity (I) of the incident particles and the number of exposed target atoms (n) as described below. The I value is a measure of time averaged energy flux (μA × min). Hence, most nuclear reactions in carbon-11 and fluorine-18 chemistry are characterized in microamperes (μA) and time of irradiation (min). The purity as an index of isotopic enrichment has to be specified since this can also affect yield (see below).

$$R = \sigma IN = \sigma Inx$$

I = number of incident particles
n = number of target atoms per cm^3
x = thickness of target in cm
σ = proportionality constant, characteristic of nuclear reactions

1.7 RADIOLABELING APPROACHES FOR CARBON-11 AND FLUORINE-18

The target nitrogen for producing carbon-11 by the $^{14}N(p,\alpha)^{11}C$ reaction is most often nitrogen gas diluted with 0.1% O_2 or 5−10% H_2 so that the main product is $[^{11}C]CO_2$ or $[^{11}C]CH_4$, respectively.[47] Due to the short half-life of carbon-11, radiochemistry with $[^{11}C]CO_2$ or $[^{11}C]CH_4$ needs to be performed immediately after production. In the case of $[^{11}C]CO_2$, radiochemistry can be performed with a Grignard

or organolithium precursor resulting in a [^{11}C]carboxylate product. However, most PET radiochemistry reactions convert [^{11}C]CO_2 or [^{11}C]CH_4 into a more reactive form, such as [^{11}C]MeI[48,49], [^{11}C]HCN[50] or [^{11}C]CO[51] . There are many efficient methods for the production of ^{11}C-labeling agents from [^{11}C]CO_2 or [^{11}C]CH_4.[45,52] However, a detailed description is outside the scope of this thesis introduction. [^{11}C]MeI, [^{11}C]HCN and [^{11}C]CO were employed as ^{11}C-labeling agents for the work in thesis.

The ^{18}O(p,n)^{18}F reaction on ^{18}O-enriched water produces fluorine-18 as aqueous [^{18}F]fluoride ion.[47] As delivered, the aqueous [^{18}F]fluoride ion has low nucleophilicity because of the surrounding waters of hydration and has to be azeotropically dried before use. There are two typical approaches to acheive this: 1) repetitively add small portions of acetonitrile to [^{18}F]fluoride ion and evaporate or 2) trap the [^{18}F]fluoride ion onto a quaternary methyl ammonium (QMA) exchange resin and release with a solution of a weak base (e.g., K_2CO_3) in slightly aqueous acetonitrile and and then evaporate. The method chosen is usually dictated by the available automation for minimizing the radiation burden to the chemist. The typical mixture used to activate [^{18}F]fluoride ion for ^{18}F-labeling experiments employs kryptofix 2.2.2®-K_2CO_3. After the drying process, the [^{18}F]fluoride ion is in a highly reactive form and can readily undergo a nucleophilic addition or substitution reaction. It is important to remember that the [^{18}F]fluoride ion is also basic and could remove an acidic proton or cause undesired elimination generating volatile [^{18}F]HF. There are many useful ^{18}F-labeling agents derived from [^{18}F]fluoride ion, which are adequately covered in a few recent review articles.[52-55] [^{18}F]Fluoromethyl bromide[56], [^{18}F]fluoromethyl bromide-d_2[57,58], [^{18}F]2-fluoroethyl bromide[59] and [^{18}F]*p*-fluoro-benzyl bromide[60] were employed as ^{18}F-labeling agents for the work in this thesis.

1.8 PET RADIOLIGAND DEVELOPMENT FOR RECEPTOR IMAGING

The development of a PET receptor radioligand can be a demanding task. However, there are several established guidelines to aid in their development. These guidelines are[61-65]:

- High brain uptake. In general, the candidate radioligand should enter the brain at > 100% SUV, where:

$$\%\ \text{SUV} = \left[\frac{\%\, injected\ activity}{brain\ tissue\,(g)} \times body\ weight\,(g) \right]$$

  %SUV normalizes for subject body weight and injected dose and therefore allows for some comparisons of results across experiments and species.

- Low non-specific binding. The candidate radioligand should allow for an adequate ratio of receptor-specific to non-specific binding.

- High affinity or potency. In general, the affinity (*i.e.*, IC_{50}, K_d or K_i,) or potency (*i.e.*, K_B) value of the candidate radioligand should be in the low to sub-nanomolar range, with the value depending on the concentration (B_{max}) value of the target protein. A useful guideline for determining the required affinity is $BP = B_{max}/K_d$, where *BP* should be about 10. IC_{50} values are converted into K_i or K_B using the Cheng and Prussoff equation[66] as shown below.

$$K_X = \frac{Y}{1+\frac{[L]}{Z}}$$

X = i or B
$Y = IC_{50}$ (50% inhibition of binding)
L = concentration of competition radioligand or agonist
$Z = K_d$ of radioligand or EC_{50} of agonist

- High selectivity. The ideal candidate radioligand should not bind to any non-target receptor or protein in vivo in a way that would interfere with biomathematical modeling.

- The molecular weight of the candidate radioligand should be < 500 g/mol to allow adequate passage through the blood-brain barrier.

- *LogP* value as an index of lipophilicity should be in the range of 2 to 3.5 to allow for adequate brain entry without excessive non-specific binding. *LogP* is the log of the solute distribution coefficient between *n*-octanol and water, described by:

$$LogP = Log\left(\frac{[solute]_{n-octanol}}{[solute]^{unionized}_{aqueous}}\right)$$

- Little or no brain entry of radiolabeled metabolites. Brain entry of radiolabeled metabolites would likely interfere with accurate PET measurements.

- Amenability to rapid labeling with a short-lived PET radioisotope (*e.g.*, ^{11}C or ^{18}F) and in adequate RCY for PET imaging experiments. In general, radiolabeling should be completed within 3 half-lives of radionuclide production.

- The radioligand should have high specific radioactivity (SR). The SR of a radioligand is defined as the ratio of radioactivity (Bq) to non-radioactive form (mol). The required SR depends on the B_{max} value of the target protein. Excessive non-radioactive molecule could competitively displace radioligand from its target binding site.

- Acceptable safety. The candidate radioligand should be toxicologically safe and suitable for injection into living subjects at tracer doses.

1.9 CANDIDATE RADIOLIGANDS

Most early attempts to image brain CB_1 receptors in vivo with PET or SPECT have relied on structural modification of rimonabant. However, **5** has high lipophilicity (*cLogP* = 6.95) and lacks an accessible site for labeling with an imaging radionuclide such as ^{11}C, ^{18}F or ^{123}I. Therefore, investigators have prepared several analogs of **5** with the aim of exploiting its core 1,5-diarylpyrazole pharmacophore for CB_1 receptor imaging. These analogs (Figure 4) include [^{123}I]AM 251 ([^{123}I]**6**)[67,68], [^{123}I]AM 281 ([^{123}I]**7**)[69,70], [^{124}I]AM 281 ([^{124}I]**7**)[69,71], [^{18}F]SR 144385 ([^{18}F]**8**)[72], [^{18}F]SR 147963

([^{18}F]**9**)[72], [^{11}C]SR 149080 ([^{11}C]**10**)[73], [^{11}C]SR 149568 ([^{11}C]**11**)[73], [^{11}C]NIDA 41087 ([^{11}C]**12**)[74,75], [^{11}C]JHU75528 ([^{11}C]**13**)[76,77] and [^{11}C]JHU75575 ([^{11}C]**14**)[77]. Out of these, the more recently reported [^{11}C]**13** and [^{11}C]**14** appear to be the more promising. The reason for the recent success of [^{11}C]**13** might be related to its favourable affinity and lipophilicity profile.[73]

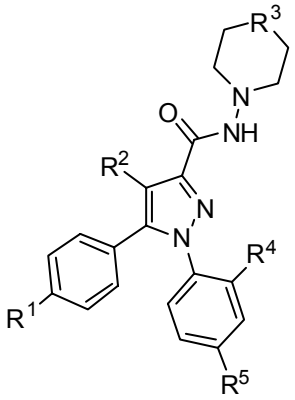

6, R^1 = I*, R^2 = Me, R^3 = CH_2, R^4 = R^5 = Cl
7, R^1 = I*, R^2 = Me, R^3 = O, R^4 = R^5 = Cl
8, R^1 = Cl, R^2 = F*CH_2, R^3 = CH_2, R^4 = R^5 = Cl
9, R^1 = Cl, R^2 = F*CH_2, R^3 = O, R^4 = R^5 = Cl
10, R^1 = Me*O, R^2 = Me, R^3 = CH_2, R^4 = R^5 = Cl
11, R^1 = Me*O, R^2 = Me, R^3 = O, R^4 = R^5 = Cl
12, R^1 = Me*O, R^2 = Me, R^3 = CH_2, R^4 = Cl, R^5 = H
13, R^1 = Me*O, R^2 = CN, R^3 = CH_2, R^4 = R^5 = Cl
14, R^1 = Me*O, R^2 = CN, R^3 = CH_2, R^4 = Br, R^5 = H

Figure 4. Structures of 1,5-diarylpyrazole candidate radioligands. Asterisks mark positions of radiolabel.

Further promising radioligands (Figure 5) are now [^{18}F]MK-9470 ([^{18}F]**15**)[78,79] and [^{11}C]MePPEP ([^{11}C]**16**)[80]. [^{18}F]**15** was developed by Merck and Co., Inc and its PET imaging results have been reported in rhesus monkey and human subjects. [^{18}F]**15** exhibits adequate brain entry, regional distribution and receptor-specific signal to be considered a suitable PET radioligand. In addition [^{18}F]**15** has acceptable radiation dosimetry.[81] However, [^{18}F]**15** displays slow brain washout, which is difficult to model. Also the extent of [^{18}F]defluorination has not been reported. After [^{18}F]defluorination any [^{18}F]fluoride ion will bind to nearby bone structures (e.g., skull) which can confound regional brain PET biomathematical modeling. In rhesus monkey, [^{11}C]**16** exhibits excellent maximal brain uptake and binds selectively to CB_1 receptors. [^{11}C]**16** is currently being assessed for suitability in human subjects but the results have not been reported yet..

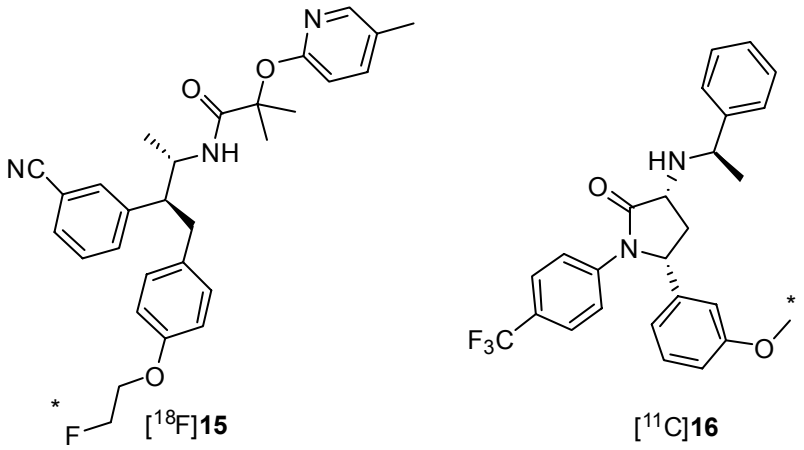

[^{18}F]**15** [^{11}C]**16**

Figure 5. Structures of [^{18}F]MK-9470 ([^{18}F]**15**) and [^{11}C]MePPEP ([^{11}C]**16**). Asterisks mark position of radiolabel.

2 PROJECT OBJECTIVE AND SUB-OBJECTIVES

The main objective of this project was to identify a radioligand suitable for in vivo imaging of brain CB_1 receptors as a tool for ascertaining their role in psychiatric and neurodegenerative disorders. This objective was to be accomplished through several sub-objectives, such as:

i. Synthesize new ligands and precursors in carrier-free form (*i.e.*, free of reference ligand) so that they would be amenable to radiolabeling with a short-lived positron-emitter (^{11}C or ^{18}F).

ii. Radiolabel the candidate ligands with a cyclotron-produced, positron-emitter (^{11}C or ^{18}F) using a remote–controlled, custom-made or commercially available radiolabeling apparatus. The radiolabeled candidate ligands were to be prepared in adequate radiochemical yield and purity for in vivo imaging experiments.

iii. Assess the candidate radioligands in monkeys with PET scanning under baseline conditions or conditions in which binding is selectively blocked by pre- or post treatment with a high dose of CB_1-selective ligand to determine brain uptake and receptor-specific signal.

iv. Identify and measure monkey plasma composition (%) of parent radioligand and radiometabolites over time with radio-HPLC

v. Submit the non-radioactive form of those candidate radioligands found to be promising in monkey for toxicological assessment, with a view to further safe study in human subjects at trace doses.

3 RESULTS AND DISCUSSION

The results of the research on the synthesis, radiolabeling and in vivo evaluation of CB_1 receptor ligands are presented here through brief summaries of seven publications that resulted from this research effort. Full copies of the published or submitted publications follow.

3.1 SYNTHESIS AND SAR OF 1,5-DIARYLPYRAZOLES FOR IN VIVO IMAGING (PAPER I)

The 1,5-diarylpyrazole structural platform has been the subject of several SAR investigations designed to elucidate an improved pharmacophore with respect to pharmacological and physiochemical parameters.[68,75,82] A subset of these studies has focused on the development of radioligands suitable for the in vivo imaging of brain CB_1 receptors.[75] Unsuccessful attempts to obtain suitable radioligands from this class of CB_1 receptor ligand platform are shown in Figure 4 and include: [^{123}I]**6**, [^{123}I]**7**, [^{124}I]**7**, [^{18}F]**8**, [^{18}F]**9**, [^{11}C]**10**, [^{11}C]**11** and [^{11}C]**12**. The failure of these radioligands in vivo was attributed to either high lipophilicity and/or inadequate binding affinity. When this study began, [^{123}I]**7** and [^{11}C]**12** were attractive lead compounds due to their high binding affinity and relatively low lipophilicity. Here we attempted to extend the existing SAR by developing ligands based on lead structures **7** and **12** (Figure 6).

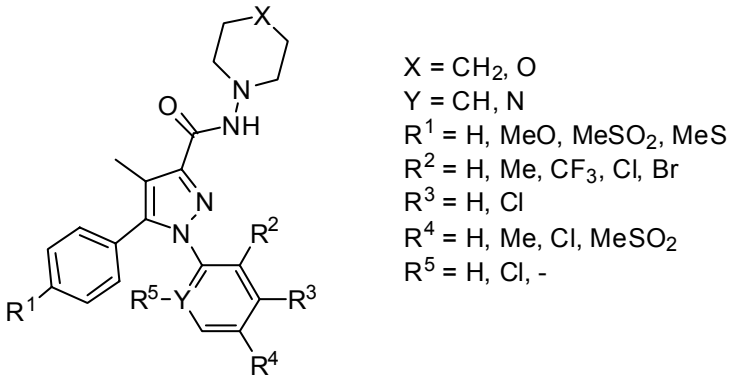

Figure 6. Structural variation of the 1,5-diarylpyrazole template.

Each ligand was synthesized from the appropriately substituted-propiophenone according to a previously established general procedure (Scheme 1)[68,75]. The ligands were evaluated for potency at CB_1 and CB_2 receptors using a [^{35}S]GTPγS functional assay[83]. *cLogP* values were calculated with Pallas 3.0 for Windows. Seventeen new ligands were synthesized. The K_B values at the CB_1 receptors ranged from 11 to > 16,000 nM, CB_1 versus CB_2 selectivities from 0.6 to 773 and *cLogP*s from 3.61 to 6.25. From this work, an interesting new ligand (**17**; Figure 6; X = CH_2, Y = C, R^1 = MeO, R^2 = Br, R^3 = R^4 = R^5 = H) emerged as a candidate for labeling with carbon-11 and in vivo imaging the CB_1 receptors. For **17**, the *cLogP*, CB_1 receptor potency (K_B value) and selectivity for binding to the CB_1 over the CB_2 receptor were 5.7, 11 nM and > 772, respectively. Based on the results from this work, **17** was selected for radiosynthesis and PET imaging experiments

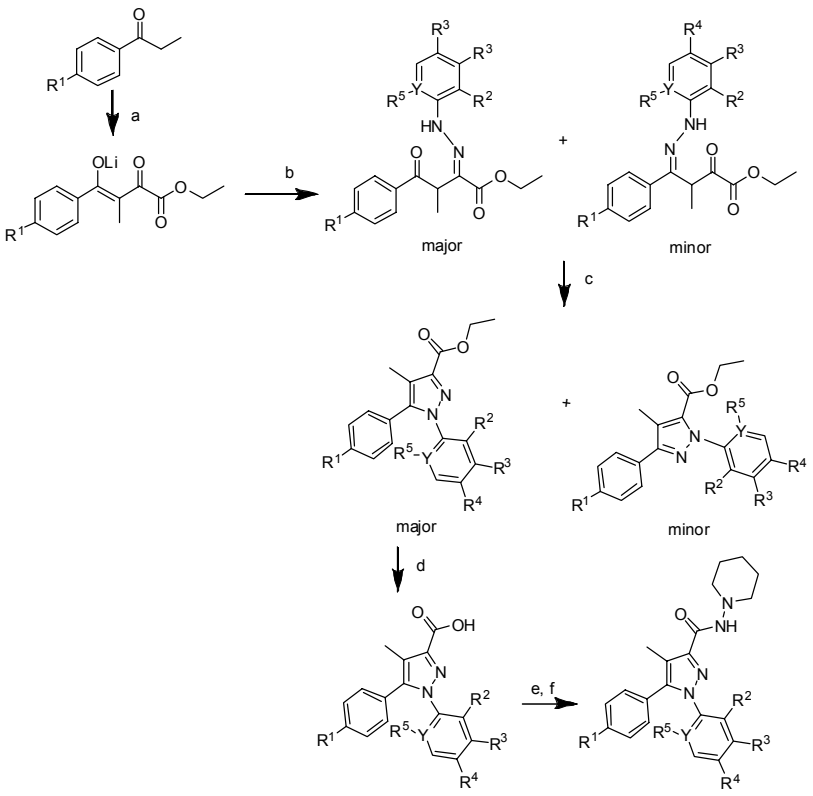

Scheme 1. Synthesis of 1,5-diarylpyrazoles. Reagents and conditions: a) LiHMDS, Et_2O, diethyl oxalate, −78 °C; b) substituted-phenylhydrazine HCl, EtOH; c) AcOH, Δ; d) KOH, MeOH; e) $SOCl_2$, toluene; f) 1-aminopiperidine, TEA, DCM.

3.2 A FACILE AND REGIOSELECTIVE SYNTHESIS OF RIMONABANT THROUGH AN ENAMINE-DIRECTED 1,3-DIPOLAR CYCLOADDITION (PAPER II)

A common method for the synthesis of the prototypical 1,5-diarylpyrazole, rimonabant, or one of its cognates is shown in Scheme 1.[68,84] This method of synthesis has many limitations. These include long reaction times, structural modification limited by the few commercially available substituted phenylhydrazines, and lack of regioselectivity. In this paper, I presented a novel regioselective synthesis of rimonabant through an enamine-directed 1,3-dipolar cycloaddition (Scheme 2).

In my new approach (Scheme 2), 4'-chloropropiophenone was converted into a morpholine enamine using $TiCl_4$ in a method introduced by White and Weingarten.[85] Separately, chloro[(2,4-dichlorophenyl)hydrazono]ethyl acetate[86], a known precursor for generating the requisite nitrile imine, was prepared from 2,4-dichloroaniline according to a previously established procedure.[86] In order to increase the reactivity of the hydrazonoyl chloride (**18**, Scheme 2), the Finkelstein reaction was used to exchange the chloro substituent (**18**, Scheme 2) with the iodo substituent (**19**, Scheme 2). Treatment of the morpholine enamine with the hydrazonoyl iodide in the presence of TEA (3 eq.) at room temperature gave **20** (Scheme 2). In order to demonstrate regioselectivity, the morpholine enamine derived from 4-chlorophenylacetone was reacted with the hydrazonoyl iodide at elevated temperature giving **22** (Scheme 2).

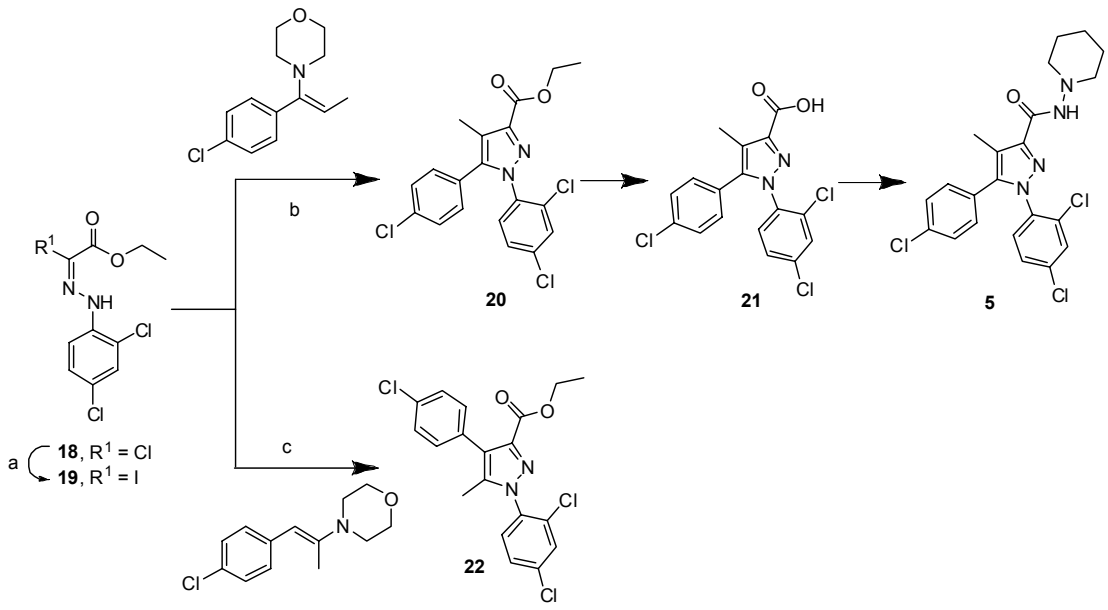

Scheme 2. New synthetic approach to 1,5-diarylpyrazole (**20**) and 1,4-diarylpyrazole (**22**) structures. Reagents, conditions and yields: a) NaI, acetone, 92%; b) TEA, DME, RT, 22%; c) TEA, toluene, Δ, 11%.

3.3 RADIOSYNTHESIS AND IN VIVO EVALUATION OF ^{11}C-LABELED 1,5-DIARYLPYRAZOLE CANDIDATE RADIOLIGANDS (PAPER III)

When this project began the candidate radioligands from the 1,5-diarylpyrazole class of CB_1 receptor ligands were largely unsuccessful. Their failures were mainly attributed to high lipophilicity and/or inadequate binding affinity. Recently, [^{11}C]**13** was reported to give a clear and marked CB_1 receptor-specific signal.[76] The reason(s) for its success were unclear. [^{11}C]**13** differed from failed [^{11}C]**10** by having a nitrile substitutuent in the 4-position of the pyrazole ring instead of a methyl substituent. Here we explored the role of this substituent exchange by preparing three radioligands (*i.e.*, [^{11}C]**12**, its bromo derivative [^{11}C]**17** and [^{11}C]**14**), each differing in substituents, lipophilicity and binding affinity, and evaluating their performance in vivo. The lipophilicities and potencies of **5**, **12**−**14** and **17** are shown below (Table 1).

Table 1. In vitro potency at CB_1 and CB_2 receptors, $cLogD_{7.4}$ and $LogD_{7.4}$ data for **5**, **12**−**14** and **17**.

Ligand	CB_1 K_B[a] (nM)	CB_2 K_B[a] (nM)	$cLogD_{7.4}$[b]	$LogD_{7.4}$
5 (SR141716A)	6.1	>6,776	7.0	4.6 ± 0.8 (n = 4)
12 (NIDA41078)	25.0	2,091	5.7	3.7 ± 0.2 (n = 6)
13 (JHU75528)	30.3	1,640	5.3	3.6 ± 0.3 (n = 6)
14 (JHU75575)	20.3	1,710	4.8	3.4 ± 0.1 (n = 6)
17	11.0	>8,500	5.9	4.2 ± 0.3 (n = 6)

[a] All values are from single determinations and have an inherent variability of three-fold. [b] $cLogD_{7.4}$ data calculated by using Pallas 3.0 for Windows.

3.3.1 Radiochemistry

Each candidate radioligand ([^{11}C]**12**, [^{11}C]**14** or [^{11}C]**17**) was prepared from its *O-desmethyl* precursor (**23**–**25**) using the "loop" method[87] with [^{11}C]iodomethane and purified with HPLC (Scheme 3). The radiosynthesis time, including formulation for each ligand, was about 40 min. The decay-corrected isolated radiochemical yields of [^{11}C]**12**, [^{11}C]**14** and [^{11}C]**17** from [^{11}C]carbon dioxide were 16 ± 12%, 5.0 ± 2.6% and 10.7 ± 2.5%, respectively. Specific radioactivies ranged from 36 to 336 GBq/μmol and radiochemical purity exceeded 99%. The obtained RCYs, SRs and purities for [^{11}C]**12**, [^{11}C]**14** and [^{11}C]**19** were adequate for PET imaging experiments.

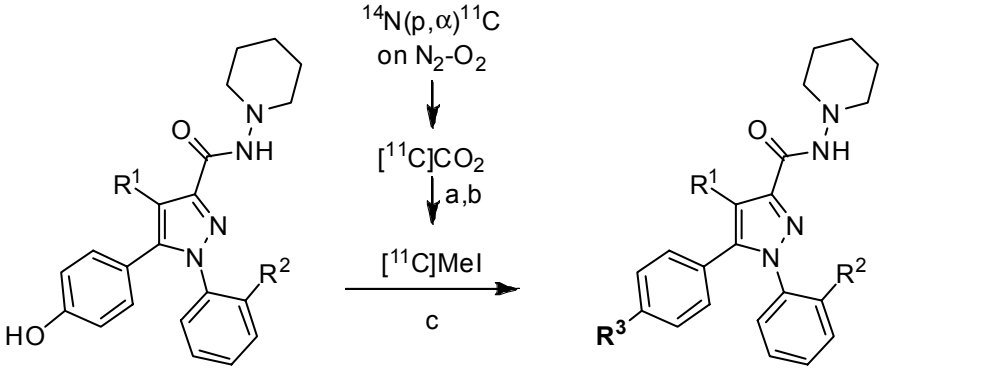

Scheme 3. Radiosynthesis of [^{11}C]**12**, [^{11}C]**14** and [^{11}C]**17**. Reagents and conditions: a) Ni-molecular sieves (4 Å), H_2, 410 °C; b) [^{11}C]CH_4, I_2, 720 °C; c) "Loop", Precursor (**23**, **24** or **25**), DMF, 0.5 M (n-Bu)$_4$NOH in MeOH, RT, ~ 5 min. Asterisks mark positions of radiolabel.

3.3.2 PET Imaging in Monkey

After injection of [^{11}C]**12**, [^{11}C]**14** or [^{11}C]**17** into monkey (Fig. 7, Panels A−C), PET showed that radioactivity distributed according to known CB_1 receptor densities. Thereafter, radioactivity in all brain regions increased for [^{11}C]**12** and [^{11}C]**17**, but declined for [^{11}C]**14** until the end of scanning (120 min). The PET images of [^{11}C]**12** and [^{11}C]**17** are likely contaminated with radiometabolite(s). These radioligands are therefore unsuitable for PET imaging of the CB_1 receptors. In contrast [^{11}C]**14** is much less likely to be contaminated with radiometabolite(s) and gives an appreciable signal in vivo.

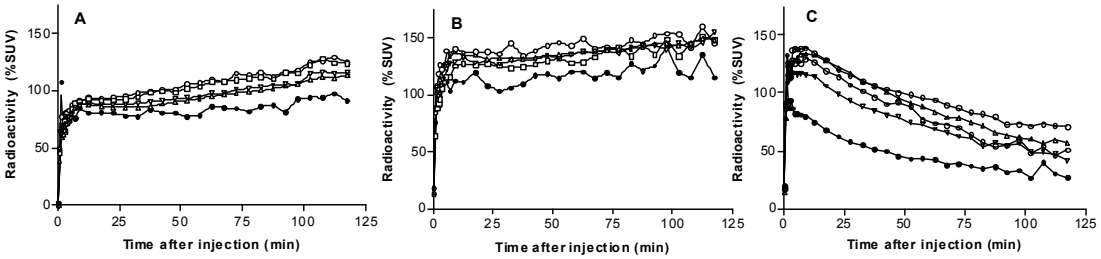

Figure 7. Regional time-radioactivity curves after *i.v.* injection of [^{11}C]**12** (Panel A), [^{11}C]**17** (Panel B) and [^{11}C]**14** (Panel C) into monkey under baseline condition. Key: ○, cerebellum; △, cortex; ▽, limbic area; □, striatum; ●, pons.

3.3.3 Plasma Measurements

Radio-HPLC of plasma showed that each radioligand was rapidly metabolized. For [^{11}C]**12** and [^{11}C]**17**, analysis of plasma in baseline and preblock experiments revealed the presence of two radiometabolite fractions with shorter retention times than the parent radioligand. Plasma for [^{11}C]**14** showed the presence of three radiometabolite fractions with shorter retention times than the parent radioligand and possibly a single more lipophilic radiometabolite fraction. These data show that [^{11}C]**12** and [^{11}C]**17** are metabolized differently to [^{11}C]**14**. This may be related to the differing substituents at the 4-position of the pyrazole ring. Hence, the promise of [^{11}C]**14** for PET imaging is likely related to favorable metabolism and a lack of brain-penetrating radioactive metabolites. [^{11}C]**14** merits further investigation for PET imaging of CB_1 receptors in human subjects.

3.4 RADIOLABELING AND IN VIVO EVALUATION OF PIPISB WITH CARBON-11 OR FLUORINE-18 (PAPERS IV & V)

N-(4-Fluoro-benzyl)-4-(3-(piperidin-1-yl)-indole-1-sulfonyl)benzamide (PipISB, **26**, Scheme 4)[88] was identified as a high potency (K_B =1.5 nM) candidate radioligand for in vivo imaging of the cannabinoid type-1 (CB_1) receptors with a relatively low computed lipophilicity (*cLogP* = 5.14).

3.4.1 Radiochemistry

Ligand **26** and precursors for radiolabeling were obtained from Eli Lilly and Co. Radiolabeling of **26** was performed by two methods (Scheme 4), method A with carbon-11 and method B with fluorine-18. In method A, [^{11}C]**26** was prepared in one step from [^{11}C]carbon monoxide, itself prepared from cyclotron-produced [^{11}C]carbon dioxide. In method B, [^{18}F]**26** was prepared from cyclotron-produced [^{18}F]fluoride ion in a four-step synthesis with [^{18}F]4-fluorobenzyl bromide as labeling agent. The total radiosynthesis time for method A was 44 min; decay-corrected isolated RCY from [^{11}C]carbon dioxide ranged from 3.1 to 11.6% and SRs from 21 to 67 GBq/μmol. The radiosynthesis time for method B was about 115 min; decay-corrected isolated RCYs from [^{18}F]fluoride ion ranged from 1.5 to 5.6% and SRs from 200 to 348 GBq/μmol. [^{11}C]**26** and [^{18}F]**26** were obtained in a radiochemical purity > 99%. The obtained

RCYs, SRs and radiochemical purities were adequate for further PET imaging experiments.

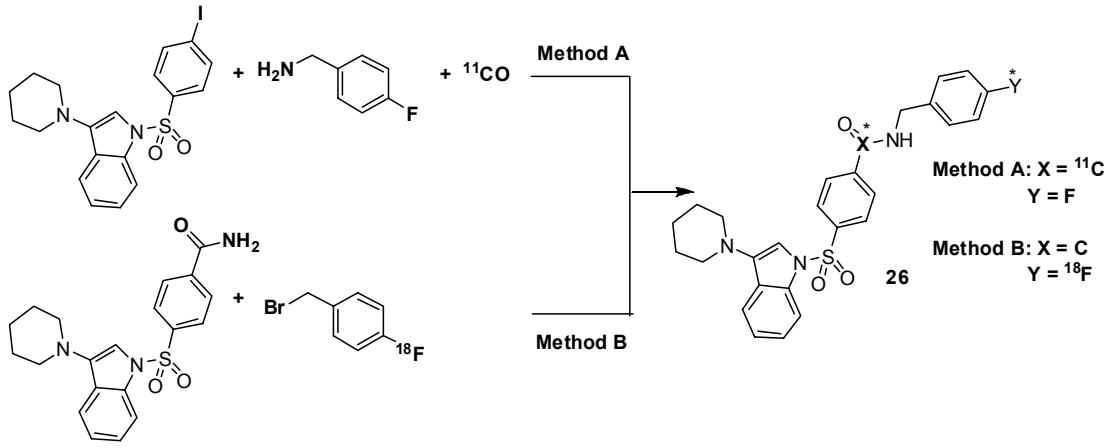

Scheme 4. Radiosyntheis of [^{11}C]PipISB ([^{11}C]**26**) and [^{18}F]PipISB ([^{18}F]**26**). Asterisks mark positions of radiolabel.

3.4.2 PET Imaging in Monkey

[^{11}C]**26** or [^{18}F]**26** was injected intravenously into rhesus or cynomolgus monkey, respectively, and examined with PET at baseline (Fig. 8, Panels A and B) and after treatment with a CB_1 receptor-selective ligand (**26** at 1 mg/kg, i.v. for [^{11}C]**26**, or 4-(3-cyclopentyl-indole-1-sulfonyl)-*N*-(tetrahydro-pyran-4-yl-methyl)-benzamide (ISPB)[86] at 1 mg/kg, i.v. for [^{18}F]**26** (Fig. 8, Panel C)). Brain radioactivity uptake was highest in striatum and cerebellum, and reached 170−270% SUV at 120 min after injection of [^{11}C]**26** and 180% SUV at 240 min after injection of [^{18}F]**26**. Radioactivity was well-retained in all CB_1 receptor-rich regions. Under CB_1 receptor pretreatment or displacement conditions, initial brain uptakes of radioactivity were similar to those at baseline conditions. Regional brain radioactivity concentrations then became homogeneous and diminished to between 70 and 80% SUV at 120 min after injection of [^{11}C]**26** and to 25% SUV at 240 min after injection of [^{18}F]**26**. Hence, [^{11}C]**26** and [^{18}F]**26** showed CB_1 receptor-specific binding in monkey brain in vivo.

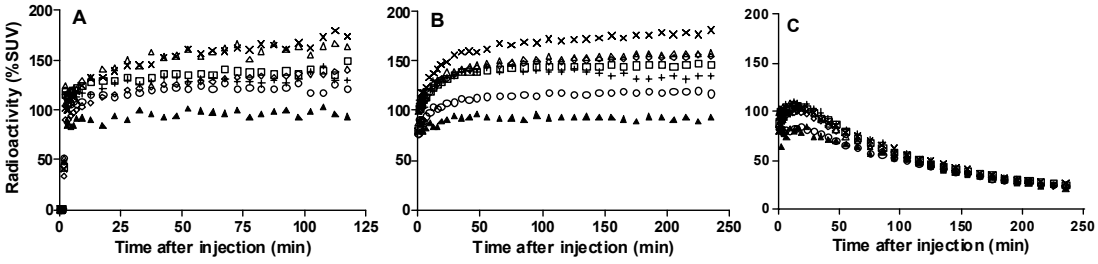

Figure 8. Regional time-radioactivity curves in monkey brain after i.v. injection of [^{11}C]**26** (Panel A), [^{18}F]**26** (Panel B), and [^{18}F]**26** after pretreatment with ISPB (1 mg/kg, i.v.) (Panel C). Key: ×, striatum; △, cerebellum; ◇, frontal cortex; □, lateral temporal cortex; +, thalamus; ○, medial temporal cortex; ▲, pons.

3.4.3 Plasma Measurements

Relative plasma concentrations of radioligand and radiometabolites were concurrently measured in baseline experiments with HPLC. [^{18}F]**26** was not defluorinated to a significant degree but was metabolized to less lipophilic radiometabolites, as was [^{11}C]**26**.

3.5 SYNTHESIS, EX VIVO EVALUATION AND RADIOLABELING OF 1,5-DIPHENYL-PYRROLIDIN-2-ONES (PAPER VI)

[^{11}C]MePPEP ([^{11}C]**16**)[80] has been reported to be a promising radioligand for PET imaging of CB_1 receptors. Four analogs (**27**, FMePPEP), 3-fluoromethoxy (**28**, FMPEP), 3-fluoromethoxy-d_2 (**29** FMPEP-d_2) and 3-fluoro-ethoxy analogs (**30**, FEPEP), derived from the 1,5-diphenyl-pyrrolidin-2-one platform of **16,** were identified as having attractive physiochemical and pharmacological properties compared to **5** (Table 2). **29** is not shown below in Table 2 because it is expected to have the same properties as **28**. Here are shown the radiolabeling of [^{11}C]**27** and [^{18}F]**28**–**30** in adequate activities for evaluation as candidate PET radioligands in vivo.

Table 2. In vitro potency at CB_1 and CB_2 receptors, CB_1 selectivity over CB_2 receptors and *cLogD*$_{7.4}$ data for **5**, **16**, **27**, **28** and **30**.

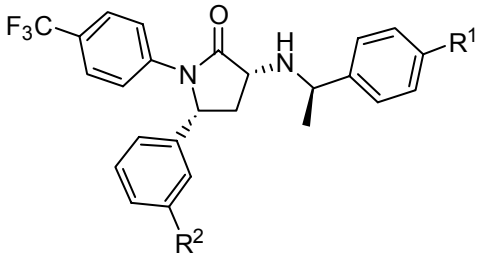

Ligand	R^1	R^2	CB_1 K_B (nM)[a]	CB_1 versus CB_2 selectivity	*cLogD*$_{7.4}$[b]
5 (rimonabant)			0.698 ± 0.200	>2,830	7.0
16 (MePPEP)	H	OCH_3	0.472 ± 0.160	769	5.7
27 (FMePPEP)	F	OCH_3	0.216 ± 0.004	2,160	5.7
28 (FMPEP)	H	OCH_2F	0.187 ± 0.018	3,580	5.7
30 (FEPEP)	H	OCH_2CH_2F	0.424 ± 0.021	>19,500	5.8

[a] All values represent mean ± SEM of three determinations. [b] *cLogD*$_{7.4}$ data calculated by using Pallas 3.0 for windows.

3.5.1 Radiochemistry

[^{11}C]**27** was prepared by treating the appropriate *O*-desmethyl precursor (**31**) with [^{11}C]iodomethane under basic conditions in a "loop" apparatus[87] (Scheme 5). After reverse phase HPLC, [^{11}C]**27** was obtained in adequate isolated decay-corrected RCY of 16.5% (n = 2) from cyclotron-produced [^{11}C]carbon dioxide with high specific radioactivity (> 261 GBq/μmol at EOS). Preparation time was about 40 min. The radiochemical purities of [^{11}C]**27** were > 95%. [^{18}F]**28**–**30** were prepared by treatment of the *O-desmethyl* precursor (**32**) with the appropriate ^{18}F-labeling agent (*i.e.* [^{18}F]FCH_2Br, [^{18}F]FD_2Br or [^{18}F]$F(CH_2)_2Br$) under basic conditions using a modified version of an automated, commercially available module (Scheme 5). After reverse phase HPLC, the final formulated product was obtained in adequate isolated decay-corrected RCY (5.9 ± 1.3% ([^{18}F]**28**; n = 3), 7.9 ± 2.5% ([^{18}F]**29**; n = 6) and 7.9 ± 2.2%

([^{18}F]**30**; n = 6) from [^{18}F]fluoride ion and in sufficiently high specific radioactivity > 57 GBq/μmol at EOS. The preparation times were about 120 min. The radiochemical purities of [^{18}F]**28**–**30** were > 95%. The obtained RCYs, SRs and radiochemical purities for [^{11}C]**27**, [^{18}F]**28**–**30** were adequate for further investigation with PET imaging.

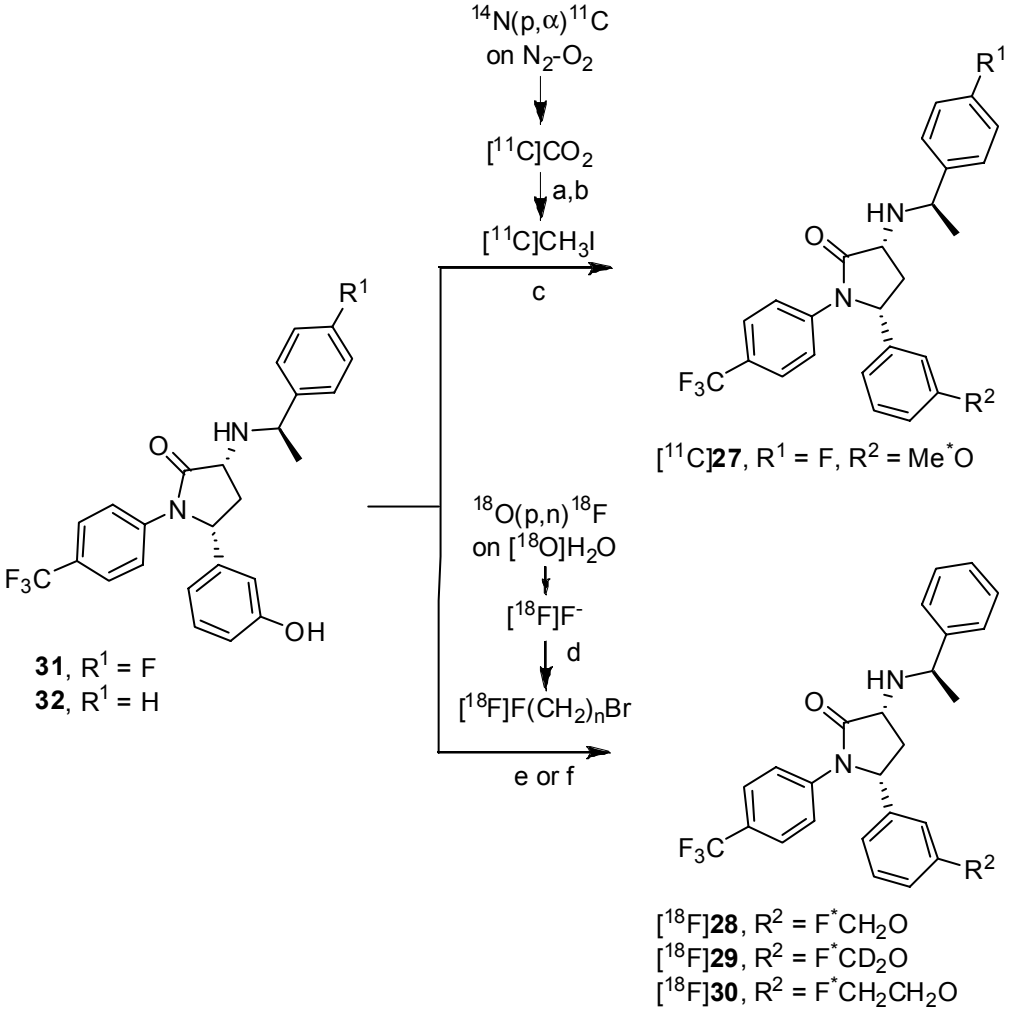

Scheme 5. Radiosynthesis of [^{11}C]FMePPEP ([^{11}C]**27**), [^{18}F]FMPEP ([^{18}F]**28**), [^{18}F]FMPEP-d_2 ([^{18}F]**29**) and [^{18}F]FEPEP ([^{18}F]**30**). Reagent and conditions: a) $Ni_{(s)}$-molecuar sieves (4Å), H_2, 410 ^oC; b) [^{11}C]CH_4, I_2, 720 ^oC; c) "Loop", DMF, 0.5 M (n-Bu)$_4$NOH in MeOH, RT, ~ 3 min, d) K 2.2.2-K^+ complex, solvent (MeCN for CH_2Br_2, CD_2Br_2 and o-dichlorobenzene for bromoethyl tosylate, Δ; e) Cs_2CO_3, DMF, Δ; f) DMF, (n-Bu)$_4$NOH in MeOH. Asterisks mark positions of radiolabel.

3.6 DISCOVERY OF 3,4-DIARYLPYRAZOLINES AS CANDIDATE RADIOLIGANDS (PAPER VII)

Here new candidate radioligands were identified from the 3,4-diarylpyrazoline CB_1 receptor antagonist platform. One candidate radioligand ([^{11}C](±)-**33**,) along with its eutomer ([^{11}C](−)-**33**, Figure 5) and distomer ([^{11}C](+)-**33**) were radiolabeled in high specific radioactivity with [^{11}C]HCN and evaluated in monkey with PET imaging. The affinities for the CB_1 and CB_2 receptors and *cLogP* data for ligands **5**, (−)-**33** and (+)-**33** are shown below (Table 3).

Table 3. IC_{50} and K_i values for the CB_1 and CB_2 receptors and *cLogP* data for ligands **5**, (−)-**33** and (+)-**33**.

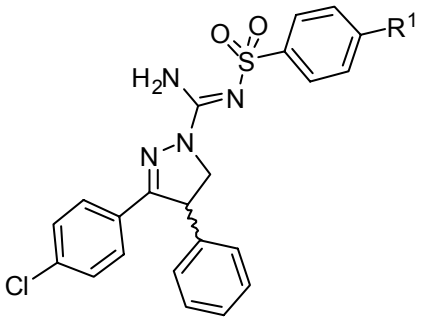

Ligand	R^1	CB_1 IC_{50} (nM)[a]	CB_2 IC_{50} (nM)[a]	CB_1 K_i (nM)[a]	CB_2 K_i (nM)[a]	*cLogP*[b]
5(rimonabant)		2.2 ± 0.5	4,570 ± 410	0.4 ± 0.1	697 ± 63	6.95
(−)-**33**	CN	2.8 ± 0.3	> 33,000	0.5 ± 0.1	> 5,000	3.85
(+)-**33**	CN	100 ± 10.0	> 33,000	16.9 ± 2.0	> 5,000	3.85

[a] Values are represent the mean ± SD of three determinations. [b] *cLogP* values were calculated by using the Pallas 3.0 software (Compudrug, USA).

3.6.1 Radiochemistry

[^{11}C]Hydrogen cyanide was produced from target [^{11}C]methane which gives higher SR than if produce from [^{11}C]carbon dioxide.[89] The radiosynthesis of [^{11}C](±)-**33** is shown in Scheme 6. The non-optimized decay-corrected isolated RCY was 36% (n = 2). The radioligand was obtained in high radiochemical purity (> 98%) and was free of precursor. Specific radioactivities were ≥ 56 GBq/μmol at time of injection. We attempted to prepare the radiolabeled [^{11}C](–)-**33** and [^{11}C](+)-**33** according to the same method. However, chiral phase HPLC of product revealed racemization had occurred during the reaction. By changing the base to KH_2PO_4, [^{11}C](–)-**33** and [^{11}C](+)-**33** were obtained in > 95% ee.

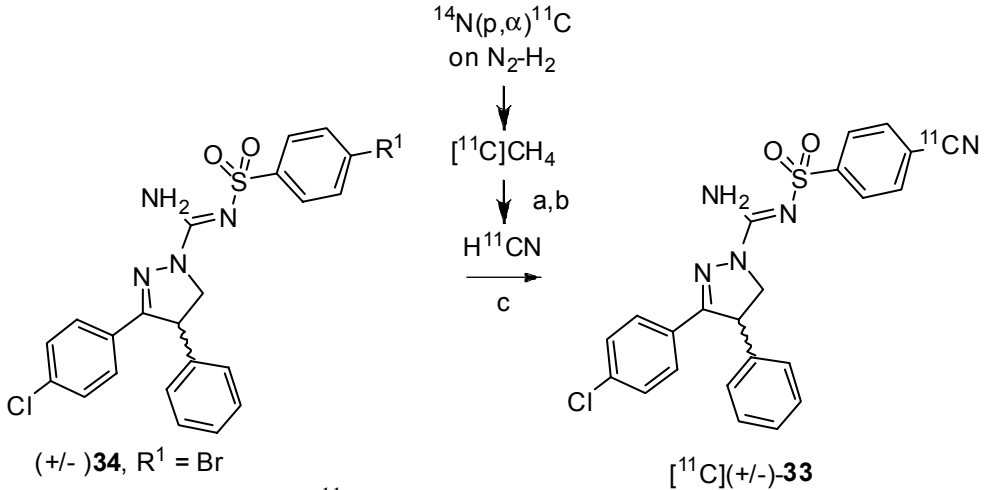

Scheme 6. Radiosynthesis of [^{11}C](±)-**33**. Conditions and reagents: a) Pt, NH_3 (20–30 mL/min), 990 °C. b) 50% H_2SO_4, 90 °C; c) precursor (**34**), $Pd(PPh_3)_4$, KOH, K2.2.2, DMSO, 110 °C.

3.6.2 PET Imaging in Monkey

The regional brain TACs of [^{11}C](−)-**33** and [^{11}C](+)-**33** are shown in Figure 9, Panels A and B. After injection of [^{11}C](−)-**33** there was high uptake and retention of radioactivity across brain according to the rank order of CB_1 receptor densities. [^{11}C](+)-**33**, failed to give a sustained CB_1 receptor-specific distribution. [^{11}C](−)-**33** was not injected into monkey under pretreatment conditions for the work in this thesis. The adequate brain uptake and regional distribution of [^{11}C](−)-**33** under baseline conditions demonstrate its promise.

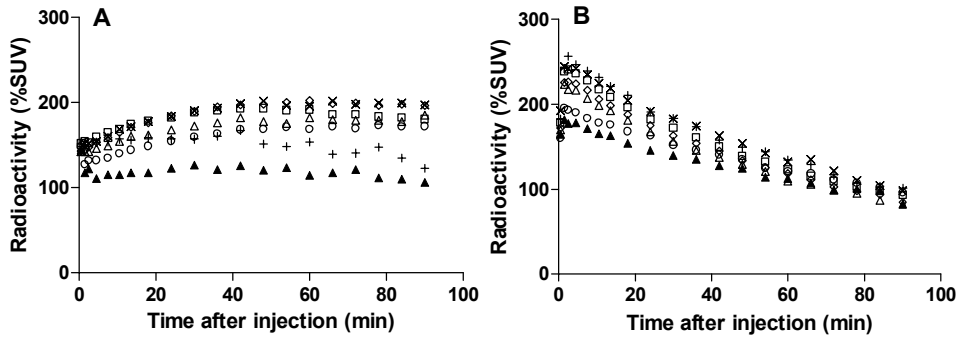

Figure 9. Regional time-radioactivity curves after i.v. injection of [^{11}C](−)-**33** (Panel A) or [^{11}C](+)-**33** (Panel B) in cynomolgus monkey under baseline conditions. Key: ×, striatum; △, cerebellum; ◇, frontal cortex; □, lateral temporal cortex; +, thalamus; ○, medial temporal cortex; ▲, pons.

3.6.3 Plasma Measurements

Analysis of venous monkey plasma from the [^{11}C](–)-**33** revealed three radiometabolites with shorter retention times (t_Rs = 2.3, 5.8 and 8 min) than the parent radioligand (t_R = 8.5 min). Unchanged radioligand declined to 50% of radioactivity in plasma at 45 min after injection. The presence of the three radiometabolite fractions slowly increased throughout the scan. The radiometablites with shorter retention times are not likely to pass the blood-brain barrier. Hence, [^{11}C](–)-**33** has favorable metabolism.

3.7 FUTURE DIRECTIONS IN APPLICATIONS OF CB_1 RADIOLIGANDS

There has been considerable progress in the development of CB_1 receptor radioligands within this thesis as well as parallel progress by other researchers. A number of radioligands are now available for imaging brain CB_1 receptors in human populations. Despite such significant advances, there are still many further potential applications and many future directions that may be taken. These include, for example:

i. Imaging psychiatric populations.[90] There have been previous attempts to image the CB_1 receptors in patients with Tourette's syndrome and schizophrenia. However, these attempts applied radioligands that were unsuitable for sensitive imaging in vivo. Application of a more promising CB_1 selective radioligand in combination with in vivo imaging would greatly enhance understanding of the role of CB_1 receptors in neuropsychiatric disorders and could help monitor progression of therapy.

ii. Drug development. The use of a suitable radioligand in combination with in vivo imaging could aid in drug development though the dose-occupancy paradigm that allows for more accurately determining the optimal dose for drug in clinical trials and for shortening the overall development and its costs.

4 CONCLUSIONS

The development of radioligands for in vivo imaging is a highly challenging task. However, a set of guidelines outlined previously has emerged to aid in their development. Here we applied those guidelines successfully to the development of radioligands suitable for in vivo imaging of CB_1 receptors. Paper I explored the existing 1,5-diarylpyrazole template of **5** to identify a candidate radioligand with an optimal potency and lipophilicity profile. **17** was identified as an attractive candidate radioligand for further investigation with PET imaging.

The synthetic procedure used in Paper I for the SAR development required several steps and long reaction times. In Paper II, a facile and regioselective synthetic procedure was identified to assist in advanced SAR development from this structural class.

During the course of this thesis, [^{11}C]**13** was identified as a suitable PET radioligand by another research group. Three [^{11}C]1,5-diarylpyrazole analogs of [^{11}C]**13**, namely ([^{11}C]**12**, [^{11}C]**17** and [^{11}C]**14**) differing in pharmacological and physiochemical profiles were prepared and imaged with PET in rhesus monkey together with plasma radiometabolite analysis (Paper III) to identify the reasons governing success or failure from this structural class. The results show that favorable metabolism conferred by a nitrile substituent in 4-position of the pyrazole ring is likely related to recent successes.

Based on attractive pharmacological/physiological parameters and amenability to radiolabeling with PET isotopes, **26** was identified as an attractive candidate radioligand. Paper IV presented the successful radiolabeling of [^{11}C]**26** and [^{18}F]**26** in adequate RCYs, SRs and purities for further investigation with PET imaging. The PET imaging outcomes of [^{11}C]**26** and [^{18}F]**26** in monkey are shown in Paper V. Each candidate radioligand demonstrated the appropriate brain regional distribution and gave a high specific signal.

In Paper VI candidate radioligands from the 1,5-diphenyl-pyrrolidin-2-one class of CB_1 receptor ligand were radiolabeled in adequate RCYs, SRs and purities for future investigation with PET imaging.

In Paper VII, one racemic 3,4-diarylpyrazoline ligand (±)-**33** along with its eutomer ((−)-**33**) and distomer ((+)-**33**) were radiolabeled from target produced [^{11}C]methane with [^{11}C]HCN in high specific radioactivity and in adequate RCY and purities. They were evaluated in monkey with PET imaging. [^{11}C](−)-**33** showed appropriate brain regional distribution and showed a high receptor-specific signal.

Through the work described is this thesis, twelve ligands were labeled with carbon-11 or fluorine-18, eight were evaluated in monkey and four of these appeared promising in monkey by showing adequate brain regional distribution and receptor-specific signal. One, [^{11}C](−)-**33,** is currently being considered for use in human subjects. The main objective of this thesis has therefore been met.

5 ACKNOWLEDGEMENTS

The work described in this thesis has been aided by direct and/or indirect contributions from many people. A list of the people I would especially like to thank follows below.

Supervisors: Professor Christer Halldin and Dr. Victor W. Pike.

Past and current members of KI radiochemistry group: Dr. Anu Airaksinen, Mr. Arsalan Amir, Mr. Jan Andersson, Mr. Guennadi Jogalov, Dr. Zisheng Jia, Mr. Sangram Nag, Mr. Carsten Steiger, Mr. Phong Troung, Dr. Raisa Krasikova, Dr. Magnus Schou, Dr. Peter Johnström, Ms. Siv Eriksson.

Past and current member of NIMH radiochemistry group: Ms. Cheryl Morse, Dr. John Musachio, Dr. Lisheng Cai, Dr. Shuiyu Lu, Ms. Penny Nolton, Mr. Jinsoo Hong, Mr. Andrew Taku, Dr. Emmanuelle Briard, Mr. Jay Shah, Dr. Julie McCarron, Ms. Kelly Sprague, Dr. Umesha Shetty, Dr. Neva Lazarova, Dr. Joon-Hyun Chun, Mr. Sebastian Temme.

Past and current members of the KI imaging group: Prof. Lars Farde, associate Prof. Balázs Gulyás, Dr. Jacqueline Borg, Dr. Simon Červenka, Dr. Nina Erixon-Lindroth, Dr. Per Karlsson, Mr. Nils Sjöholm, Mr. Sjoerd Finnema, Dr. Stefan Pauli, Dr. Andrea Varrone, Dr. Katarina Varnäs, Dr. Hristina Jovanovic, Dr. Judit Sóvágó, Mr. Julio Gabriel, Dr. Zolt Cselényi, Dr. Akihiro Takano, Dr. Sari Karlsson.

Past and current member of NIH imaging group: Dr. Robert B. Innis, Dr. Vanessa Cropley, Dr. Masanori Ichise, Dr. Sami S. Zoghbi, Mr. Robert L. Gladding, Dr. Fumihiko Yasuno, Ms. Mette Skinbjerg, Mr. Garth Terry, Dr. Jeih-San Liow, Dr. Masahiro Fujita, Mr. Ed Tuan, Mr. Jonathan Gourley.

Past and current members of Eli Lilly and Co.: Dr. John M. Schaus, Mr. Joseph H Krushinski, Dr. Lee A. Phebus, Mr. Eyassu Chernet, Dr. Stephen A. Hitchcock, Dr. Christian C. Felder and Ms. Amy K. Chesterfield.

Members of the Karolinska Pharmacy PET radiochemistry group: Prof. Sharon Stone-Elander, Dr. Jan-Olov Thorell, Dr. Anna Fredriksson, Erik Samen and Erik Engström.

Project assistants: Ms. Ulla-Kajsa Perhsson and Ms. Karin Zahir.

Past and current KI nurses: Mr. Johan Mohlin, Mr. Jan Everhov, Ms. Kjerstin Lind and Ms. Gudrun Nylén.

Computer support: Mr. Urban Hansson

Family: Joyce, John, Maura, Eric

Financial support from the NIH (NIMH) Intramural Research Program and the KI-NIH Graduate Partnership Program in Neuroscience.

NIH Clinical PET center for performing cyclotron irradiations.

6 REFERENCES

1. Lambert, D. M. Les vertus du cannabis à travers les millenaires (The virtues of cannabis through the millenium). *J. Pharm. Belg*. **2001**, *56*, 111–118.

2. Mechoulam, R., *The Pharmacohistory of Cannabis Sativa*; CRC Press: Boca Raton, Fl, 1986; pp 1–19.

3. El Sohly, M. Cannabis and cannabinoids. In *Pharmacology, Toxicology, and Therapeutic Potential*. Grotenhermen, F; Russo, E., Eds.; Haworth Press: New York, 2002; pp 27–36.

4. Gaoni, Y.; Mechoulam, R. Isolation structure and partial synthesis of active constituent of hashish. *J. Am. Chem. Soc*. **1964**, *86*, 1646–1647.

5. Mechoulam, R.; Gaoni, Y. The absolute configuration of Δ^1-tetrahydrocannabinol, the major active constituent of hashish. *Tetrahedron Lett*. **1967**, *12*, 1109−1111.

6. Johnson, M. R.; Melvin, L. S. *Cannabinoids as Therapeutic Agents*. CRC Press: Boca Raton, FL, 1986; pp 121–145.

7. Devane, W. A.; Dysarz, F. A.; Johnson, M. R.; Melvin, L. S.; Howlett, A. C. Determination and characterization of a cannabinoid receptor in rat-brain. *Molecular Pharmacology* **1988**, *34*, 605−613..

8. Munro, S.; Thomas, K. L.; Abushaar, M. Molecular characterization of a peripheral receptor for cannabinoids. *Nature* **1993**, *365*, 61–65.

9. Shire, D.; Carillon, C.; Kaghad, M.; Calandra, B.; Rinaldi-Carmona, M.; Le Fur, G.; Caput, D.; Ferrara, P. An amino-terminal variant of the central cannabinoid receptor resulting from alternative splicing. *J. Biol. Chem*. **1995**, *270*, 3726–3731.

10. Ryberg, E.; Vu, H. K.; Larsson, N.; Groblewski, T.; Hjorth, S.; Elebring, T.; Sjorgren, S.; Greasley, P. J. Identification and characterisation of a novel splice variant of the human CB_1 receptor. *FEBS Lett*. **2005**, *579*, 259–264.

11. Howlett, A. C.; Barth, F.; Bonner, T. I.; Cabral, G.; Casellas, P.; Devane, W. A.; Felder, C. C.; Herkenham, M.; Mackie, K.; Martin, B. R.; Mechoulam, R.; Pertwee, R. G. International Union of Pharmacology. XXVII. Classification of cannabinoid receptors. *Pharmacol. Rev*. **2002**, *54*, 161–202.

12. Ross, R. A. Anandamide and vanilloid TRPV1 receptors. *Br. J. Pharmacol*. **2003**, *140*, 790–801.

13. Hirst, R. A.; Almond, S. L.; Lambert, D. G. Characterisation of the rat cerebella CB_1 receptor using SR141716A, a central cannabinoid receptor antagonist. *Neurosci. Lett*. **1996**, *220*, 101–104.

14. Dewar, K. M.; Montreuil, B.; Grondin, L.; Reader, T. A. Dopamine D_2 receptors labeled with [^{3}H]raclopride in rat and rabbit brains. Equilibrium binding, kinetics, distribution and selectivity. *J. Pharmacol. Exp. Ther*. **1989**, *250*, 696–706.

15. Herkenham, M.; Lynn, A. B.; Little, M. D.; Johnson, M. R.; Melvin, L. S.; Decosta, B. R.; Rice, K. C. Cannabinoid receptor localization in brain. *Proc. Natl. Acad. Sci. U.S.A*. **1990**, *87*, 1932–1936.

16. Herkenham, M.; Lynn, A. B.; Johnson, M. R.; Melvin, L. S.; De Costa, B. R.; Rice, K. C. Characterization and localization of cannabinoid receptors in rat-brain: a quantitative in vitro autoradiographic study. *J. Neurosci*. **1991**, *11*, 563–583.

17. Glass, M.; Dragunow, M.; Faull, R. L. Cannabinoid receptors in the human brain: a detailed anatomical and quantitative autoradiographic study in the fetal, neonatal and adult human brain. *Neuroscience* **1997**, *77*, 299–318.

18. Lynn, A. B.; Herkenham, M. Localization of cannabinoid receptors and nonsaturable high-density cannabinoid binding-sites in peripheral-tissues of the rat: Implications for receptor-mediated immune modulation by cannabinoids. *J. Pharmacol. Exp. Ther*. **1994**, *268*, 1612–1623.

19. Griffin, G.; Fernando, S. R.; Ross, R. A.; McKay, N. G.; Ashford, M. L. J.; Shire, D.; Huffman, J. W.; Yu, S.; Lainton, J. A. H.; Pertwee, R. G. Evidence for the presence of CB_2-like cannabinoid receptors on peripheral nerve terminals. *Eur. J. Pharmacol*. **1997**, *339*, 53–61.

20. Gong, J. P.; Onaivi, E. S.; Ishiguro, H.; Liu, Q. R.; Tagliaferro, P. A.; Brusco, A.; Uhl, G. R. Cannabinoid CB_2 receptors: immunohistochemical localization in rat brain. *Brain Res*. **2006**, *1071*, 10–23.

21. Van Sickle, M. D.; Duncan, M.; Kingsley, P. J.; Mouihate, A.; Urbani, P.; Mackie, K.; Stella, N.; Makriyannis, A.; Piomelli, D.; Davison, J. S.; Marnett, L. J.; Di Marzo, V.; Pittman, Q. J.; Patel, K. D.; Sharkey, K. A. Identification and functional characterization of brainstem cannabinoid CB_2 receptors. *Science* **2005**, *310*, 329–332.

22. Devane, W. A.; Hanus, L.; Breuer, A.; Pertwee, R. G.; Stevenson, L. A.; Griffin, G.; Gibson, D.; Mandelbaum, A.; Etinger, A.; Mechoulam, R. Isolation and structure of a brain constituent that binds to the cannabinoid receptor. *Science* **1992**, *258*, 1946–1949.

23. Mechoulam, R.; Benshabat, S.; Hanus, L.; Ligumsky, M.; Kaminski, N. E.; Schatz, A. R.; Gopher, A.; Almog, S.; Martin, B. R.; Compton, D. R.; Pertwee, R. G.; Griffin, G.; Bayewitch, M.; Barg, J.; Vogel, Z. Identification of an endogenous 2-monoglyceride, present in canine gut, that binds to cannabinoid receptors. *Biochem. Pharmacol*. **1995**, *50*, 83–90.

24. Sugiura, T.; Kondo, S.; Sukagawa, A.; Nakane, S.; Shinoda, A.; Itoh, K.; Yamashita, A.; Waku, K. 2-Arachidonoylgylcerol: a possible endogenous cannabinoid receptor-ligand in brain. *Biochem. Biophys. Res. Comm*. **1995**, *215*, 89–97.

25. Porter, A. C.; Sauer, J. M.; Knierman, M. D.; Becker, G. W.; Berna, M. J.; Bao, J.; Nomikos, G. G.; Carter, P.; Bymaster, F. P.; Leese, A. B.; Felder, C. C. Characterization of a novel endocannabinoid, virodhamine, with antagonist activity at the CB_1 receptor. *J. Pharmacol. Exp. Ther*. **2002**, *301*, 1020–1024.

26. Huang, S. M.; Bisogno, T.; Trevisani, M.; Al-Hayani, A.; De Petrocellis, L.; Fezza, F.; Tognetto, M.; Petros, T. J.; Krey, J. F.; Chu, C. J.; Miller, J. D.; Davies, S. N.; Geppetti, P.; Walker, J. M.; Di Marzo, V. An endogenous capsaicin-like substance with high potency at recombinant and native vanilloid VR1 receptors. *Proc. Natl. Acad. Sci. U.S.A*. **2002**, *99*, 8400–8405.

27. Howlett, A. C. The cannabinoid receptors. *Prostaglandins Other Lipid Mediat*. **2002**, *68–69*, 619–631.

28. Felder, C. C.; Dickason-Chesterfield, A. K.; Moore, S. A. Cannabinoids biology: the search for new therapeutic targets. *Mol. Interv*. **2006**, *6*, 149–161.

29. Rhee, M. H.; Bayewitch, M.; Avidor-Reiss, T.; Levy, R.; Vogel, Z. Cannabinoid receptor activation differentially regulates the various adenylyl cyclase isozymes. *J. Neurochem*. **1998**, *71*, 1525–1534.

30. Mackie, K.; Lai, Y.; Westenbroek, R.; Mitchell, R. Cannabinoids activate an inwardly rectifying potassium conductance and inhibit Q-type calcium currents in AtT20 cells transfected with rat brain cannabinoid receptor. *J. Neurosci*. **1995**, *15*, 655–661.

31. Pacher, P.; Bátkai, S.; Kunos, G. The endocannabinoid system as an emerging target of pharmacotherapy. *Pharmacol. Rev*. **2006**, *58*, 389–462.

32. Navarro, M.; Hernandez, E.; Munoz, R. M.; del Arco, I.; Villanua, M. A.; Carrera, M. R.; Rodriguez de Fonseca, F. Acute administration of the CB_1 cannabinoid receptor antagonist SR 141716A induces anxiety-like responses in the rat. *Neuroreport* **1997**, *8*, 491–496.

33. Hill, M. N.; Ho, W. S.; Sinopoli, K. J.; Viau, V.; Hillard, C. J.; Gorzalka, B. B. Involvement of the endocannabinoid system in the ability of long-term tricyclic antidepressant treatment to suppress stress-induced activation of the hypothalamic-pituitary-adrenal axis. *Neuropsychopharmacology* **2006**, *31*, 2591–2599.

34. De Vries, T. J.; Schoffelmeer, A. N. Cannabinoid CB_1 receptors control conditioned drug seeking. *Trends Pharmacol. Sci*. **2005**, *26*, 420–426.

35. Walker, J. M.; Huang, S. M. Cannabinoid analgesia. *Pharmacol. Ther*. **2002**, *95*, 127–135.

36. Pertwee, R. G. Cannabinoids and multiple sclerosis. *Pharmacol. Ther*. **2002**, *95*, 165–174.

37. Lastres-Becker, I.; Cebeira, M.; de Ceballos, M. L.; Zeng, B. Y.; Jenner, P.; Ramos, J. A.; Fernández-Ruiz, J. J. Increased cannabinoid CB_1 receptor binding and activation of GTP-binding proteins in the basal ganglia of patients with Parkinson's syndrome and of MPTP-treated marmosets. *Eur. J. Neurosci*. **2001**, *14*, 1827–1832.

38. Lastres-Becker, I.; De Miguel, R.; Fernández-Ruiz, J. J. The endocannabinoid system and Huntington's disease. *Curr Drug Targets CNS Neurol Disord* **2003**, 2, 335–347.

39. Grotenhermen, F. Cannabinoids. *Curr. Drug Targets CNS Neurol. Disord*. **2005**, *4*, 507–530.

40. Berry, E. M.; Mechoulam, R. Tetrahydrocannabinol and endocannabinoids in feeding and appetite. *Pharmacol. Ther*. **2002**, *95*, 185–190.

41. Müller-Vahl, K. R.; Schneider, U.; Koblenz, A.; Jöbges, M.; Kolbe, H.; Daldrup, T.; Emrich, H. M. Treatment of Tourette's syndrome with Δ^9-tetrahydrocannabinol (THC): a randomized crossover trial. *Pharmacopsychiatry* **2002**, *35*, 57–61.

42. Rinaldi-Carmona, M.; Barth, F.; Heaulme, M.; Shire, D.; Calandra, B.; Congy, C.; Martinez, S.; Maruani, J.; Neliat, G.; Caput, D.; Ferrara, P.; Soubrié, P.; Brelière, J.-C.; Le Fur, G. SR141716A, a potent and selective antagonist of the brain cannabinoid receptor. *FEBS Lett*. **1994**, *350*, 240–244.

43. Black, S. C. Cannabinoid receptor antagonists and obesity. *Curr. Opin. Investig. Drugs* **2004**, *5*, 389–394.

44. Balerio, G. N.; Aso, E.; Maldonado, R. Role of the cannabinoid system in the effects induced by nicotine on anxiety-like behaviour in mice. *Psychopharmacology (Berl)* **2006**, *184*, 504–513.

45. Ametamey, S. M.; Honer, M.; Schubiger, P. A. Molecular imaging with PET. *Chem. Rev.* **2008**, DOI:10.1021/cr0782426.

46. Lieser, K. H. *Nuclear and Radiochemistry*. Wiley-VCH: Weinheim, 2001.

47. Qaim, S. M.; Clark, J. C.; Crouzel, C.; Guillaume, M.; Helmeke, H. J.; Nebeling, B.; Pike, V. W.; Stöcklin, G. PET radionuclide production. In *Radiopharmaceuticals for Positron Emission Tomography*. Stöcklin, G.; Pike, V. W., Eds.; Kluwer Academic Publishers: Dordrecht, Netherlands, 1993; pp 1–33.

48. Långström, B.; Lundqvist, H., Preparation of ^{11}C-methyl iodide and its use in synthesis of ^{11}C-methyl-L-methionine. *Int. J. Appl. Radiat. Isot.* **1976**, *27*, 357–363.

49. Larsen, P.; Ulin, J.; Dahlstrom, K.; Jensen, M., Synthesis of [^{11}C]iodomethane by iodination of [^{11}C]methane. *Appl. Radiat. Isot.* **1997**, *48*, 153–157.

50. Christman, D. R.; Finn, R. D.; Karlstrom, K. I.; Wolf, A. P. Production of ultra high activity ^{11}C-labeled hydrogen cyanide, carbon dioxide, carbon monoxide and methane via ^{14}N(p,α)^{11}C reaction. *Intl. J. Appl. Radiat. Isot.* **1975**, *26*, 435−442.

51. Kihlberg, T.; Långström, B, Biologically active ^{11}C-labeled amides using palladium-mediated reactions with aryl halides and [^{11}C]carbon monoxide. *J. Org. Chem.* **1999**, *64*, 9201–9205.

52. Brady, F.; Clark, J. C.; Luthra, S. K. Building on a 50-year legacy of the MRC Cyclotron Unit: the Hammersmith radiochemistry pioneering journey. *J. Label. Compd. Radiopharm.* **2007**, *50*, 903–926.

53. Coenen, H. H. Fluorine-18 labeling methods: features and possibilities of basic reactions. In *PET Chemistry*. Schubiger, P. A.; Lehmann, L.; Friebe, M., Eds.; Springer-Verlag: Heidelberg, 2007; pp 15–50.

54. Cai, L.; Lu, S.; Pike, V. W. The chemistry of ^{18}F-fluoride ion. *Eur. J. Org. Chem.* **2008**, DOI: 10.1002/ejoc.200800114.

55. Snyder, S. E.; Kilbourn, M. R.; Chemistry of fluorine-18 radiopharmaceuticals. In *Handbook of Radiopharmaceuticals*. Welch, M. J.; Redvanley, C. S., Eds.; John Wiley & Sons: West Sussex, England, 2003; pp 195–227.

56. Coenen, H. H.; Colosimo, M.; Schuller, M.; Stocklin, G. Preparation of n.c.a. [^{18}F]CH_2BrF via aminopolyether supported nucleophilic-substitution. *J. Label. Compd. Radiopharm.* **1986**, *23*, 587–595.

57. Schou, M.; Halldin, C.; Sovago, J.; Pike, V. W.; Hall, H.; Gulyas, B.; Mozley, P. D.; Dobson, D.; Shchukin, E.; Innis, R. B.; Farde, L. PET evaluation of novel radiofluorinated reboxetine analogs as norepinephrine transporter probes in the monkey brain. *Synapse* **2004**, *53*, 57–67.

58. Hamill, T. G.; Burns, H. D.; Eng, W. S.; Ryan, C.; Krause, S.; Gibson, R.; Hargreaves, R. An improved fluorine-18 labeled neurokinin-1 receptor ligand. *Mol. Imaging Biol.* **2002**, *4* (Supp. 1), 34.

59. Iwata, R.; Pascali, C.; Bogni, A.; Furumoto, S.; Terasaki, K.; Yanai, K. [^{18}F]Fluoromethyl triflate, a novel and reactive [^{18}F]fluoromethylating agent:

preparation and application to the on-column preparation of [^{18}F]fluorocholine. *Appl. Radiat. Isot*. **2002**, *57*, 347–352.

60. Hatano, K.; Ido, T.; Iwata, R. The synthesis of ortho-[^{18}F]fluorobenzyl and para-[^{18}F]fluorobenzyl bromides and their application to the preparation of labeled neuroleptics. *J. Label. Compd. Radiopharm*. **1991**, *29*, 373–380.

61. Waterhouse, R. N. Determination of lipophilicity and its use as a predictor of blood-brain barrier penetration of molecular imaging agents. *Mol. Imaging Biol*. **2003**, *5*, 376–389.

62. Laruelle, M.; Slifstein, M.; Huang, Y. Relationships between radiotracer properties and image quality in molecular imaging of the brain with positron emission tomography. *Mol. Imaging Biol*. **2003**, *5*, 363–375.

63. Pike, V. W. Positron-emitting radioligands for studies in vivo: probes for human psychopharmacology. *J. Psychopharmacology* **1993**, *7*, 139–158.

64. Halldin, C.; Gulyás, B; Farde, L. PET studies with carbon-11 radioligands in neuropsychopharmacological drug development. *Curr. Pharm. Des*. **2001**, *7*, 1907–1929.

65. Halldin, C.; Gulyás, B.; Langer, O.; Farde, L. Brain radioligands: state of the art and new trends. *Q. J. Nucl. Med*. **2001**, *45*, 139–152.

66. Cheng, Y.; Prusoff, W. H. Relationship between the inhibition constant (K_1) and the concentration of inhibitor which causes 50 per cent inhibition (IC_{50}) of an enzymatic reaction. *Biochem. Pharmacol*. **1973**, *22*, 3099–3108.

67. Gatley, S. J.; Gifford, A. N.; Volkow, N. D.; Lan, R.; Makriyannis, A. ^{123}I-labeled AM251: a radioiodinated ligand which binds in vivo to mouse brain cannabinoid CB_1 receptors. *Eur. J. Pharmacol*. **1996**, *307*, 331–338.

68. Lan, R.; Liu, Q.; Fan, P.; Lin, S.; Fernando, S. R.; McCallion, D.; Pertwee, R.; Makriyannis, A. Structure-activity relationships of pyrazole derivatives as cannabinoid receptor antagonists. *J. Med. Chem*. **1999**, *42*, 769–776.

69. Gatley, S. J.; Lan, R.; Volkow, N. D.; Pappas, N.; King, P.; Wong, C. T.; Gifford, A. N.; Pyatt, B.; Dewey, S. L.; Makriyannis, A. Imaging the brain marijuana receptor: development of a radioligand that binds to cannabinoid CB_1 receptors in vivo. *J. Neurochem*. **1998**, *70*, 417–423.

70. Berding, G.; Müller-Vahl, K.; Schneider, U.; Gielow, P.; Fitschen, J.; Stuhrmann, M.; Harke, H.; Buchert, R.; Donnerstag, F.; Hofmann, M.; Knoop, B. O.; Brooks, D. J.; Emrich, H. M.; Knapp, W. H. [^{123}I]AM281 single-photon emission computed tomography imaging of central cannabinoid CB_1 receptors before and after Δ^9-tetrahydrocannabinol therapy and whole-body scanning for assessment of radiation dose in Tourette patients. *Biol. Psychiatry* **2004**, *55*, 904–915.

71. Berding, G.; Schneider, U.; Gielow, P.; Buchert, R.; Donnerstag, F.; Brandau, W.; Knapp, W. H.; Emrich, H. M.; Muller-Vahl, K. Feasibility of central cannabinoid CB_1 receptor imaging with [^{124}I]AM281 PET demonstrated in a schizophrenic patient. *Psychiatry Res*. **2006**, *147*, 249–256.

72. Mathews, W. B.; Scheffel, U.; Finley, P.; Ravert, H. T.; Frank, R. A.; Rinaldi-Carmona, M.; Barth, F.; Dannals, R. F. Biodistribution of [^{18}F]SR144385 and [^{18}F]SR147963: selective radioligands for positron emission tomographic studies of brain cannabinoid receptors. *Nucl. Med. Biol*. **2000**, *27*, 757–762.

73. Mathews, W. B.; Scheffel, U.; Rauseo, P. A.; Ravert, H. T.; Frank, R. A.; Ellames, G. J.; Herbert, J. M.; Barth, F.; Rinaldi-Carmona, M.; Dannals, R. F. Carbon-11 labeled radioligands for imaging brain cannabinoid receptors. *Nucl. Med. Biol.* **2002**, *29*, 671–677.

74. Kumar, J. S.; Prabhakaran, J.; Arango, V.; Parsey, R. V.; Underwood, M. D.; Simpson, N. R.; Kassir, S. A.; Majo, V. J.; Van Heertum, R. L.; Mann, J. J. Synthesis of [*O*-methyl-^{11}C]1-(2-chlorophenyl)-5-(4-methoxyphenyl)-4-methyl-1*H*-pyrazole- 3-carboxylic acid piperidin-1-ylamide: a potential PET ligand for CB1 receptors. *Bioorg. Med. Chem. Lett.* **2004**, *14*, 2393–2396.

75. Katoch-Rouse, R.; Pavlova, O. A.; Caulder, T.; Hoffman, A. F.; Mukhin, A. G.; Horti, A. G. Synthesis, structure-activity relationship, and evaluation of SR141716 analogues: development of central cannabinoid receptor ligands with lower lipophilicity. *J. Med. Chem.* **2003**, *46*, 642–645.

76. Horti, A. G.; Fan, H.; Kuwabara, H.; Hilton, J.; Ravert, H. T.; Holt, D. P.; Alexander, M.; Kumar, A.; Rahmim, A.; Scheffel, U.; Wong, D. F.; Dannals, R. F. ^{11}C-JHU75528: A radiotracer for PET imaging of CB_1 cannabinoid receptors. *J. Nucl. Med.* **2006**, *47*, 1689–1696.

77. Fan, H.; Ravert, H. T.; Holt, D. P.; Dannals, R. F.; Horti, A. G. Synthesis of 1-(2,4-dichlorophenyl)-4-cyano-5-(4-[^{11}C]methoxyphenyl)-*N*-(piperidin-1-yl)-1*H*-pyrazole-3-carboxamide ([^{11}C]JHU75528) and 1-(2-bromophenyl)-4-cyano-5-(4-[^{11}C]methoxyphenyl)-*N*-(piperidin-1-yl)-1*H*-pyrazole-3-carboxamide ([^{11}C]JHU75575) as potential radioligands for PET imaging of cerebral cannabinoid receptor. *J. Label. Compd. Radiopharm.* **2006**, *49*, 1021–1036.

78. Burns, H. D.; Van Laere, K.; Sanabria-Bohorquez, S.; Hamill, T. G.; Bormans, G.; Eng, W. S.; Gibson, R.; Ryan, C.; Connolly, B.; Patel, S.; Krause, S.; Vanko, A.; Van Hecken, A.; Dupont, P.; De Lepeleire, I.; Rothenberg, P.; Stoch, S. A.; Cote, J.; Hagmann, W. K.; Jewell, J. P.; Lin, L. S.; Liu, P.; Goulet, M. T.; Gottesdiener, K.; Wagner, J. A.; de Hoon, J.; Mortelmans, L.; Fong, T. M.; Hargreaves, R. J. [^{18}F]MK-9470, a positron emission tomography (PET) tracer for *in vivo* human PET brain imaging of the cannabinoid-1 receptor. *Proc. Natl. Acad. Sci. U.S.A.* **2007,** *104*, 9800–9805.

79. Liu, P.; Lin, L. S.; Hamill, T. G.; Jewell, J. P.; Lanza, T. J.; Gibson, R. E.; Krause, S. M.; Ryan, C.; Eng, W. S.; Sanabria, S.; Tong, X. C.; Wang, J. Y.; Levorse, D. A.; Owens, K. A.; Fong, T. M.; Shen, C. P.; Lao, J. L.; Kumar, S.; Yin, W. J.; Payack, J. F.; Springfield, S. A.; Hargreaves, R.; Burns, H. D.; Goulet, M. T.; Hagmann, W. K. Discovery of *N*-{(1*S*,2*S*)-2-(3-cyanophenyl)-3-[4-(2-[^{18}F]fluoroethoxy)phenyl]-1-methylpropyl}-2-methyl-2-[(5-methylpyridin-2-yl)oxy]propanamide, a cannabinoid-1 receptor positron emission tomography tracer suitable for clinical use. *J. Med. Chem.* **2007**, *50*, 3427–3430.

80. Yasuno, F.; Brown, A. K.; Zoghbi, S. S.; Krushinski, J. H.; Chernet, E.; Tauscher, J.; Schaus, J. M.; Phebus, L. A.; Chesterfield, A. K.; Felder, C. C.; Gladding, R. L.; Hong, J.; Halldin, C.; Pike, V. W.; Innis, R. B. The PET radioligand [^{11}C]MePPEP binds reversibly and with high specific signal to cannabinoid CB_1 receptors in nonhuman primate brain. *Neuropsychopharmacology* **2008**, *33*, 259–269.

81. Van Laere, K.; Koole, M.; Sanabria Bohorquez, S. M.; Goffin, K.; Guenther, I.; Belanger, M. J.; Cote, J.; Rothenberg, P.; De Lepeleire, I.; Grachev, I. D.; Hargreaves, R. J.; Bormans, G.; Burns, H. D. Whole-body biodistribution and radiation dosimetry of the human cannabinoid type-1 receptor ligand ^{18}F-MK-9470 in healthy subjects. *J. Nucl. Med.* **2008**, *49*, 439–445.

82. Francisco, M. E. Y.; Seltzman, H. H.; Gilliam, A. F.; Mitchell, R. A.; Rider, S. L.; Pertwee, R. G.; Stevenson, L. A.; Thomas, B. F. Synthesis and structure-activity relationships of amide and hydrazide analogues of the cannabinoid CB_1 receptor antagonist *N*-(piperidinyl)-5-(4-chlorophenyl)-1-(2,4-dichlorophenyl)-4-methyl-1*H*-pyrazole-3-carboxamide (SR141716). *J. Med. Chem*. **2002**, *45*, 2708–2719.

83. DeLapp, N. W.; McKinzie, J. H.; Sawyer, B. D.; Vandergriff, A.; Falcone, J.; McClure, D.; Felder, C. C. Determination of [^{35}S]guanosine-5'-*O*-(3-thio)triphosphate binding mediated by cholinergic muscarinic receptors in membranes from Chinese hamster ovary cells and rat striatum using an anti-G protein scintillation proximity assay. *J. Pharmacol. Exp. Ther*. **1999**, *289*, 946–955.

84. Kotagiri, V. K.; Suthrapu, S.; Reddy, J. M.; Rao, C. P.; Bollugoddu, V.; Bhattacharya, A.; Bandichhor, R. An improved synthesis of rimonabant: anti-obesity drug. *Org. Process Res. Develop*. **2007**, *11*, 910–912.

85. White, W. A.; Weingarten, H. A versatile new enamine synthesis. *J. Org. Chem*.**1967**, *32*, 213–214.

86. Barth, F.; Congy, C.; Martinez, S.; Rinaldi-Carmona, M. 4-Cyanopyrazole-3-carboxamide derivatives preparation and therapeutic application thereof. *PCT Int. App. WO*2005000820, 2005.

87. Wilson, A. A.; Garcia, A.; Jin, L.; Houle, S. Radiotracer synthesis from [^{11}C]-iodomethane: a remarkably simple captive solvent method. *Nucl. Med. Biol*. **2000**, *27*, 529–532.

88. Allen, J. R.; Amegadzie, A. K.; Gardinier, K. M.; Gregory, G. S.; Hitchcock, S. A.; Hoogestraat, P. J.; Jones, W. D., Jr.; Smith, D. L. Preparation of arylsulfonyl-substituted indoles as CB_1 receptor modulators. *PCT Int. App. WO*2005066126, 2005.

89. Andersson, J.; Troung, P.; Amir, A.; Halldin, C. In-target produced [^{11}C]methane increases specific radioactivity. *J. Label. Compd. Radiopharm*. **2007**, *50* (supp.1), 106.

90. Van Laere, K. In vivo imaging of the endocannabinoid system: a novel window to a central modulatory mechanism in humans. *Eur. J. Nucl. Med. Mol. Imaging* **2007**, *34*, 1719–1726.